REPORT DOCUMENTATION PAGE

Form Approved
OMB No 0704-0188

1. AGENCY USE ONLY (Leave blank)	2. REPORT DATE	3. REPORT TYPE AND DATES COVERED
	31 December 1996	Final 01 June 1993 - 31 October 1996

4. TITLE AND SUBTITLE
Synthesis and Characterization of CuO Superconductors with Anomalous Transitions above 200 K

5. FUNDING NUMBERS
F~~49620-93-1-0321~~
61103D
3484/US

6. AUTHOR(S)
Lowell E. Wenger
J.T. Chen

7. PERFORMING ORGANIZATION NAME(S) AND ADDRESS(ES)
Wayne State University
Department of Physics
666 W. Hancock Ave.
Detroit, MI 48202

AFOSR-TR-97
0058

9. SPONSORING/MONITORING AGENCY NAME(S) AND ADDRESS(ES)
U.S. Air Force
AFOSR/NE
Building 410
Bolling AFB, DC 20332-6448

10. SPONSORING/MONITORING AGENCY REPORT NUMBER
F49620-93-1-0321

11. SUPPLEMENTARY NOTES

12a. DISTRIBUTION/AVAILABILITY STATEMENT
UNCLASSIFIED / UNLIMITED
Approved for public release; distribution unlimited.

12b. DISTRIBUTION CODE

19970128 180

13. ABSTRACT *(Maximum 200 words)*

This final report describes our continual superconductivity research on the materials and structural phases responsible for the above 200-K superconducting transitions, their synthesis conditions, and the study of the physical properties associated with these transitions. These transitions are characterized by resistive drops and flux-trapping hysteretic behavior in the magnetization measurements. Information on the magnetic properties of a reproducible flux-trapping phenomenon occurring at 336 K as well as on the synthesis conditions and structural features of multi-phase YBaCuO samples which exhibit this phenomenon are detailed. Also studies of the Josephson properties on YBaCuO single crystals are presented which indicate intrinsic Josephson junctions at the inter- and intra-unit-cell length scales. This latter result has astrong implication for atomic-plane 2-dimensional superconductivity in the cuprate superconductors. In addition, studies of the paramagnetic Meissner effect on Nb disks and cuprate samples indicate that the effect is not an intrinsic property, but dependent upon the sample geometry and the surface microstructure.

14. SUBJECT TERMS	15. NUMBER OF PAGES
Superconductivity Room-temperature superconductivity YBaCuO superconductors	52 16. PRICE CODE

17. SECURITY CLASSIFICATION OF REPORT	18. SECURITY CLASSIFICATION OF THIS PAGE	19. SECURITY CLASSIFICATION OF ABSTRACT	20. LIMITATION OF ABSTRACT
UNCLASSIFIED	UNCLASSIFIED	UNCLASSIFIED	UNLIMITED

TABLE OF CONTENTS

1. *SUMMARY*

1.1 OBJECTIVES

The primary objectives of this superconducting research effort over the past three years have been:

(1) to understand the nature of the resistive and magnetic transitions observed near room-temperature,

(2) to identify the material conditions responsible for these transitions, and

(3) to improve the material characteristics as well as its properties.

Other more fundamental issues have arisen during the course of our investigations which have led to the inclusion of the following objectives as well:

(4) to investigate the nature of unusual magnetic phenomena including the paramagnetic Meissner effect and

(5) to study the properties associated with intrinsic Josephson junctions in the cuprate superconductors.

The progress in attaining these objectives is presented in the next sections.

1.2 HIGHLIGHTS

Since our previous annual technical reports described in more detail our superconductivity research activity on materials responsible for the above 200-K superconducting transitions, their synthesis conditions, and their physical properties, we will only highlight the primary results accomplished during the past three years in this section.

(i) The electrical and magnetic characterizations of near-room-temperature phenomena in multi-phase YBaCuO ceramic samples:

- improved reproducibility of phenomena by utilizing high-pressure oxygen measuring atmosphere.

(ii) The electrical and magnetic characterizations of near-room-temperature phenomena in nominal $YBa_2Cu_3O_{7-\delta}$ single crystals:

- electrical transitions suggest two superconducting phases at 280 K and 340 K which are dependent upon the current bias and self-magnetic fields
- zero-field-cooled magnetization (ZFCM) is more diamagnetic than the field-cooled-magnetization (FCM)
- the difference between the FCM and ZFCM decreases with increasing magnetic field strength with the ZFCM/H data approaching the FCM/H.

(iii) The synthesis and material characterizations of the phase responsible for reproducible flux-trapping phenomena at 336 K in multiphase YBaCuO ceramic samples:

- systematic DTA/TG studies indicate required synthesis conditions
- DTA/TG and XRD studies suggest an oxygen-deficient, non-123 YBaCuO phase is responsible for 336-K transition.

(iv) The magnetic characterization of the flux-trapping hysteretic behavior observed in the vicinity of 336 K:

- the difference between the FCM and ZFCM decreases with increasing magnetic field strength with the ZFCM/H data approaching the FCM/H data
- the appearance of a weak ferromagnetic-like, field-cooled-magnetization (FCM) being consistent with a canted antiferromagnetic order of the Cu moments.

(v) The elimination and induction of the paramagnetic Meissner effect (PME) in Nb disks reproducibly:

- the PME is not unique to cuprate superconductors
- the observation that the PME is dependent upon the surface microstructure, sample geometry, and surface pinning
- the PME is neither an intrinsic property of the superconductors nor related to the symmetry of the order parameter.

(vi) The existence of intrinsic Josephson junctions in $YBa_2Cu_3O_{7-\delta}$ single crystals

- modulations in dynamic resistance observed as a function of magnetic field
- junction spacings from flux quantization conditions are indicative of intra- and inter-unit-cell lengths in $YBa_2Cu_3O_{7-\delta}$

1.3 PUBLICATIONS

M.S.M. Minhaj, J. Obien, D-C. Ling, J.T. Chen, and L.E. Wenger, "Magnetization studies of near-room-temperature phenomenon in CuO-based materials", *J. of Supercond.* **7**, 715 (1994).

M.S.M. Minhaj, David J. Thompson, L.E. Wenger, and J.T. Chen, "Paramagnetic Meissner effect in a niobium disk", *Physica C* **235-240**, 2519 (1994).

D-C. Ling, K. Chang, J.T. Chen, and L.E. Wenger, "Observation of microwave induced dc voltages in a $YBa_2Cu_3O_{7-\partial}$ single crystal", *Physica C* **235-240**, 3291 (1994).

David J. Thompson, M.S.M. Minhaj, L.E. Wenger, and J.T. Chen, "Observation of paramagnetic Meissner effect in niobium disks", *Phys. Rev. Lett.* **75**, 529 (1995).

D.C. Ling, J.T. Chen, Grace Yong, and L.E. Wenger, "Experimental evidence for intra- and inter-unit-cell Josephson junctions in a $YBa_2Cu_3O_{7-\delta}$ single crystal", *Phys. Rev. Lett.* **75**, 2011 (1995).

D.C. Ling, J.T. Chen, and L.E. Wenger, "Microwave-induced dc voltages in a $YBa_2Cu_3O_{7-\delta}$ single crystal", *Phys. Rev. B* **53**, 15300 (1996).

David J. Thompson, L.E. Wenger, and J.T. Chen, "Inducing and enhancing the paramagnetic Meissner effect in Nb disks", *Czech. J. of Physics* **46**, S3-1195 (1996).

J.T. Chen, D.C. Ling, and L.E. Wenger, "Intrinsic Josephson junctions in $YBa_2Cu_3O_{7-\delta}$ single crystals", *Czech. J. of Physics* **46**, S3-1257 (1996).

David J. Thompson, L.E. Wenger, and J.T. Chen, "Inducing the paramagnetic Meissner effect in Nb disks by surface ion implantation", *Phys. Rev. B* **54**, 16096 (1996).

David J. Thompson, L.E. Wenger, and J.T. Chen, "The paramagnetic Meissner effect in conventional Nb superconductors", *J. Low Temp. Physics* **105**, 509 (1996).

1.4 PRESENTATIONS

Papers presented:

American Physical Society meeting, 21-25 March 1994, Pittsburgh, PA.

- "Observation of a 336-K transition in mixed-phase YBaCuO samples", J. Obien, M.S.M. Minhaj, David J. Thompson, L.E. Wenger, and J.T. Chen.
- "Microwave effects in $YBa_2Cu_3O_{7-\delta}$ single crystals", D-C. Ling, K. Chang, J.T. Chen, and L.E. Wenger.

Spring Meeting of the Ohio Section of the APS, 13-14 May 1994, Cleveland, OH.

- "Paramagnetic Meissner Effect in a niobium disk", M.S.M. Minhaj, David J. Thompson, L.E. Wenger, and J.T. Chen.
- "Observation of magnetic-field interference patterns in a $YBa_2Cu_3O_{7-\delta}$ single crystal", D-C. Ling, Grace Yong, J.T. Chen, and L.E. Wenger.

International Conference of Materials & Mechanisms of Superconductivity - High Temperature Superconductivity - IV, Grenoble, France, 5-9 July 1994.

- "Paramagnetic Meissner effect in a niobium disk", M.S.M. Minhaj, David J. Thompson, L.E. Wenger, and J.T. Chen.
- "Observation of microwave induced dc voltages in a $YBa_2Cu_3O_{7-\delta}$ single crystal", D-C. Ling, K. Chang, J.T. Chen, and L.E. Wenger.

American Physical Society meeting, 20-24 March 1995, San Jose, CA.

- "Superconducting-like flux-trapping behavior in multi-phase YBaCuO above 300 K" M.S.M. Minhaj, David J. Thompson, J.M. Obien, J.T. Chen, and L.E. Wenger.
- "Paramagnetic Meissner effect in Nb disks", David J. Thompson, M.S.M. Minhaj, L.E. Wenger, and J.T. Chen.
- "Synthesis conditions for multi-phase YBaCuO samples exhiviting near-room-temperature flux trapping phenomena", J.M. Obien, David J. Thompson, J.T. Chen, and L.E. Wenger.

1995 Taiwan International Conference on Superconductivity, Hualien, Taiwan, R.O.C., 8-11 August 1995.

- "Evidence for intrinsic Josephson junctions in a $YBa_2Cu_3O_{7-\delta}$ single crystal", D.C. Ling, J.T. Chen, and L.E. Wenger. (Invited paper)

American Physical Society meeting, St. Louis, MO, 22 March 1996.

- "Paramagnetic Meissner effect in conventional and high-T_c superconductors" L.E. Wenger (Invited talk).
- "Enhancing the paramagnetic Meissner effect in Nb disks", David J. Thompson, L.E. Wenger, and J.T. Chen.

International Conference on the Physics and Chemistry of Molecular and Oxide Superconductors (MOS'96), Karlsruhe, Germany, 1-6 August 1996.

- "Paramagnetic Meissner effect in conventional Nb superconductors", David J. Thompson, L.E. Wenger, and J.T. Chen. (Invited oral presentation)

XXI International Conference on Low Temperature Physics, Prague, Czech Republic, 8-14 August 1996.

- "Inducing and enhancing the paramagnetic Meissner effect in Nb disks", David J. Thompson, L.E. Wenger, and J.T. Chen. (Invited oral presentation)
- "Intrinsic Josephson junctions in $YBa_2Cu_3O_{7-\delta}$ single crystals", J.T. Chen, D.C. Ling, L.E. Wenger, and J.T. Chen.

Seminars and Colloquium presented:

David J. Thompson

- "Observation of Paramagnetic Meissner Effect in Nb Disks", Seminar, Wayne State University, Detroit, MI , 3 October 1995.
- "Paramagnetic Meissner Effect in High- T_c and Conventional Superconductors Disks", Colloquium, Andrews University, Berrien Springs, MI 12 April 1996.

L.E. Wenger

- "Search for Room-Temperature Superconductivity" University of Michigan, Ann Arbor, MI, 1 February 1994.
- "Evidence for Room-Temperature Superconductivity" University of Utah, Salt Lake City, UT, 17 February 1994.
- "High-Temperature Superconductivity Research" Wright Laboratories, WPAFB, Dayton, OH, 16 March 1994.
- "The Quest for Room Temperature Superconductors", Purdue University, West Lafayette, IN, 30 September 1994.
- "Paramagnetic Meissner Effect: Evidence for d-Wave Superconductivity or Just an Extrinsic Superconducting Property?", Colloquium, Western Michigan University, Kalamazoo, MI, 2 April 1996.

J.T. Chen

- "Present Status of Superconducting-like Anomalies in Cuprates above 200 K", Seminar, Texas Center for Superconductivity, University of Houston, TX, 4 November 1994.
- "Evidence for Intrinsic Josephson Junctions in High- T_c Superconducting Cuprates" Colloquium, Wayne State University, Detroit, MI, September 1995.

1.5 PERSONNEL (01 June 1993 - 31 October 1996)

Principal Investigators:	Lowell E. Wenger, Professor of Physics J.T. Chen, Professor of Physics
Doctoral Students: (salary support)	David J. Thompson (AFOSR-93-1-0321) Grace Yong Jonathan Obien M.S.M. Minhaj D.-C. Ling
Degrees Awarded:	M.S.M. Minhaj, Ph.D. Thesis Title: "Fabrication and Magnetic Characterization of Layered Superconductors" 14 October 1994
	D-C. Ling, Ph.D. Thesis Title: "An Investigation of Electrodynamic Properties of High-T_c Superconducting $YBa_2Cu_3O_{7-\delta}$ Single Crystals" 15 December 1994
	Jonathan M. Obien, Ph.D. Thesis Title: "Synthesis and Characetrization of YBaCuO Materials Exhibiting a Magnetic Anomaly at 336 K" 13 October 1996
	David J. Thompson, Ph.D. Thesis Title: "Studies of the Paramagnetic Meissner Effect inNb Disks" 7 November 1996
	Grace J. Yong, Ph.D. Thesis Title: "An Investigation of Anomalous Resistive Transitions in $YBa_2Cu_3O_{7-\delta}$ Single Crystals " 26 November 1996

2. *STUDIES ON CERAMIC MULTI-PHASE YBaCuO SAMPLES*

In our studies on ceramic multi-phase YBaCuO samples, one critical condition for observing and reproducing a zero-resistance transition having a T_c above 200 K is to keep the specimen in an O_2 environment continuously during the electrical measurements as it is thermally cycled through the transition temperature. However in other experiments, such as microwave and magnetization measurements, anomalous high-T_c phenomena can be observed even when the specimens are not kept in an oxygen environment. One possible explanation for these different experimental observation conditions is that diffusion of oxygen molecules into a solid at room temperature is limited. Thus this process results in only the material near the surfaces of grains being affected by the oxygen diffusion and the formation of the higher-T_c material. In the microwave and magnetization measurements, disconnected granular shells can still contribute to an observable signal even though flux trapping can dominate the magnetization response. However, the observation of zero-resistance requires a continuous path of these "good" surfaces, i.e., good connectivity between the granular shells of the higher-T_c material. In order to determine the effect of low-temperature oxygen diffusion on the granular YBaCuO materials, the resistance of several multi-phase $Y_5Ba_6Cu_{11}O_y$ ceramic samples were monitored over time while continuously being maintained in an O_2 gas at 2 to 10 atms of pressure and temperatures up to 380 K. Typically, the resistance of the samples decreased at room temperature with decreases as large as an order of magnitude. Also the temperature dependence below 300 K changes from linear to a concave upwards behavior, a clear indication of a material change caused by the low-temperature oxidation. (See Fig. 2-1.) This oxidation results from an increase in the volume fraction of the higher-T_c superconducting phase and an increase in the conductivity of the intergranular regions, both contributing to overall resistance decrease. However repeated thermal cyclings can also have a deleterious effect on the intergranular coupling as the thermal expansion and contraction between grains can result in poorer mechanical contact. We believe this later effect can dominate the measured resistance in the ceramic YBaCuO samples and prevents electrical measurements from showing zero-resistance transitions more frequently in these samples.

Even though there is difficulty in observing zero-resistance transitions in these multi-phase ceramic samples, indications of superconductivity by the appearance of a hysteretic behavior between the zero-field-cooled-magnetization (ZFCM) and the field-cooled-magnetization (FCM) are observed more frequently. However these magnetic results are

less conclusive for a superconducting transition since a truly diamagnetic response below these higher transition temperatures has not been observed to date. During the period of this report, one-third of the nominal $Y_5Ba_6Cu_{11}O_y$ ceramic samples measured in our SQUID magnetometer exhibited a hysteretic behavior near room temperatures. This hysteretic behavior is typified by a weak, temperature-dependent divergence of the ZFCM from the more paramagnetic-like FCM. (See Fig. 2-2.) The FCM above 100 K can be totally accounted for by adding the magnetic contributions from the major crystalline phases found in these 5:6:11 samples ($YBa_2Cu_3O_7$, Y_2BaCuO_5, and CuO) and from the sample holder. Thus the differences in the ZFCM from the FCM can be attributed to other minority phases in the sample, including higher-T_c superconducting phases. For such a superconducting phase in a predominately paramagnetic host material, one would expected that the ZFCM to be less paramagnetic than the FCM since a small diamagnetic response would be generated by the induced shielding currents (flux exclusion) when the magnetic field is applied after cooling below T_c in zero field. Likewise no detection of the superconducting transition in the FCM measurements would be expected since flux trapping in these thin and probably discontinuous superconducting granular surfaces would cancel the diamagnetic shielding contribution.

One of the ceramic $Y_5Ba_6Cu_{11}O_y$ samples after a lengthy high-pressure oxygen anneal (over 10 atm O_2 for nearly one month at 100°C) exhibited a more distinctive, superconducting-like transition at 310 K for two different magnetic fields as shown in Fig. 2-3. The ZFCM deviates from the paramagnetic-like FCM over a 10-K temperature range and maintains a nearly constant diamagnetic difference from the FCM at lower temperatures, as if the ZFCM response simply consists of a diamagnetic response from a small "bulk-like" superconductor and a paramagnetic response from a much larger non-superconducting material. In addition, there are discontinuities (jumps) in the ZFCM data in the temperature range between 270 K and 290 K. These discontinuities always tend to go from a more diamagnetic response at lower temperatures to a more positive response at higher temperatures, very reminiscent to flux jumps observed in some inhomogeneous superconducting materials.

In summary, the aforementioned electrical and magnetic features near room temperature are consistent with superconducting transitions in multi-phase samples where the nonsuperconducting regions dominate the overall measured responses. These properties are consistent with thin material phases that reside on or near the surfaces of the 1-2-3

granules. In fact, these phases may be the result of an interfacial region having a thickness of 1 to 10 nm. This thickness would result in very small critical currents and thus explain the difficulty in observing zero-resistance transition. Similarly, this thickness would be substantially less than the penetration depth and correspondingly suppress the diamagnetic response in the magnetization measurements. Until this higher-T_c superconducting phase can be synthesized in a greater volume fraction in these ceramic samples, the reproducibility of zero-resistance transitions and clear diamagnetic transitions will be quite small. A more successful approach is suggested in the next section describing our work on nominal $YBa_2Cu_3O_{7-\delta}$ single-crystal samples.

3. *STUDIES ON NOMINAL $YBa_2Cu_3O_{7-\delta}$ SINGLE CRYSTAL SAMPLES*

As we first reported in 1991, we have observed a strong anisotropic behavior in the electrical resistance on several nominal $YBa_2Cu_3O_{7-\delta}$ single crystal samples grown in our laboratory.[1] This anisotropic behavior is characterized by the resistance along the *c* -axis exhibiting a semiconducting-like temperature dependence until 90 K where the well-known superconducting transition of the 1-2-3 superconducting phase occurs, while zero-resistance transitions are observed in the 240 K to 270 K range for currents along the surfaces (*a-b* plane) of these crystalline samples. Since the oxidation studies on the ceramic YBaCuO samples indicated surface oxidation may lead to the observation of near-room-temperature resistive transitions, we have performed more electrical and magnetic measurements on nominal single crystals during this contract period.

Extensive electrical measurements on nearly twenty crystal samples in oxygen pressures as high as 10 atms indicate the importance of maintaining an O_2 environment around the sample during the measurements, especially if reproducible resistive transitions are to be observed near room temperature. Secondly, extreme care must be taken while cooling the sample through the transition region as flux trapping can occur which can lower the T_c, diminish the size of the resistive change, or even eliminate the observation of the resistive transition as the higher resistance state is maintained. The flux trapping not only occurs because of the presence of stray magnetic fields but also by self-fields generated by external bias currents or thermal emfs. Consequently, slow cooling of the sample through the transition in the absence of any current is the preferred technique for performing electrical measurements.

Two crystals from two different batches measured in 1 atm of O_2 exhibited small bumps or changes in slope in the vicinity of 280 K which indicated some electrical property change; however, the data was inconclusive as to whether these features could be associated with a superconducting transition or not. Five other samples measured in 10 atm of O_2 clearly show resistive changes in the vicinity of 340 K and 280 K. The resistive data for one particular sample (#GY0026D-2) could be fairly well understood in terms of two superconducting transition temperatures. The 340-K transition was observable in the plane of the crystalline platelet sample and only during the warming cycle after cooling in zero current. (See Fig. 3-1.) A high-resistance state of approximately 2 Ω can easily dominate the lower-temperature measured resistive features if a bias current was applied before cooling through the transition. The resistive transition at 280 K showed a hysteretic behavior with a lower T_c measured during the cooling cycle and a larger T_c during the warming cycle as shown in Fig. 3-2. These features are very analogous to the hysteretic behavior observed in a weak-link superconductor or a conventional Josephson junction with a very small critical current. The presence of a bias current in these weak superconducting junctions can create a large enough self-field to lower the transition temperature or even completely suppress the transition. Consequently we speculate that both of these transitions are superconducting in nature even though the resistance never actually goes to zero. This interpretation is further supported by the magnetization studies which showed a hysteretic behavior between the zero-field-cooling and field-cooling measurements developing at similar temperatures.

Of 13 nominal single crystal samples measured in the SQUID magnetometer, four exhibited near-room-temperature hysteretic behavior, i.e., the zero-field-cooled-magnetization (ZFCM) is more diamagnetic than the field-cooled-magnetization (FCM) below the transition temperature as clearly shown in Fig. 3-3 for an applied field of 100 Oe. However, it should be pointed out that the magnetization for most of those samples not exhibiting a hysteretic behavior were performed in fields of less than 5 Oe which might be too small of a field for the sensitivity necessary to detect a difference between the ZFCM and the FCM responses. For two samples including one from a single crystal batch exhibiting near-room-temperature resistive transitions, the magnetic hysteresis developed at about 310 K with an uncertainty of $\pm$ 10 K due to instrumental scatter of the data. For fields between 50 and 250 Oe, the FCM/H data (FCM divided by the applied magnetic field H) are essentially the same; however, the ZFCM/H data are independent of field for lower

field strengths and for the larger fields increase towards the FCM/H data resulting in a smaller hysteresis as shown in Fig. 3-3. Thus the ZFCM/H becomes less diamagnetic with respect to the FCM/H for increasing field strengths even though the overall magnetic response is positive in sign. This behavior is qualitatively similar to the magnetic susceptibility for an inhomogeneous superconductor where ZFCM/H has its maximum diamagnetic response for the lowest field strengths and decreases towards zero for larger fields when the field is greater than the lower critical field H_{c1}. The FCM/H is always less diamagnetic than the corresponding ZFCM/H and can even be zero for low fields if the flux trapping is nearly equal to the diamagnetic flux exclusion response due to the increasing viscous nature of flux with decreasing temperature. For granular superconducting samples, the FCM/H is typically one-third of the maximum ZFCM/H result; however, this fraction can be substantially reduced if the superconducting sample has large interior regions of non-superconducting areas and strong pinning sites as is the probable case for the nominal single crystal samples.

Figure 3-4 shows the magnetic behavior of a third sample (#GY0026D-2) which is the same one exhibiting the resistive drops at 280 K and 340 K shown in Figs. 3-1 and 3-2. The ZFCM/H and FCM/H results are qualitatively similar to those described in the preceding paragraph, except the hysteresis begins in the vicinity of 340 K and the ZFCM/H and FCM/H at 500 Oe nearly coincide. Although the sign of the magnetic responses are positive, the relative magnetization changes between the ZFCM/H and the FCM/H show a diamagnetic-like character. This diamagnetic character can be further enhanced by noting that the FCM/H data for 500 Oe can be fit to the normal-state susceptibility measured for a single-phase 1-2-3 sample as indicated by the solid lines in these figures. Thus not only does the ZFCM/H data indicate the presence of a diamagnetic response below 340 K, but the FCM/H data for the lower fields is also diamagnetic in nature and becomes more diamagnetic for lower field strengths as well. The magnetization results for another nominal single crystal sample (#GY0026D-1) from the same batch exhibited nearly identical behavior for similar field strengths. The overall similarity of this magnetic behavior to that for an inhomogeneous superconductors supports the conclusion that these crystalline samples have a superconducting phase with a T_c near 340 K, in agreement with the electrical measurements.

4. *STUDIES ON MATERIALS EXHIBITING A 336-K TRANSITION*

As reported in an earlier annual reports, unusual magnetic transitions have been observed at 336 K for three different batches of granular YBaCuO samples. These transitions are characterized by the zero-field-cooled-magnetization (ZFCM) being featureless with only a weak temperature dependence in the range of 300 K to 360 K while the field-cooled-magnetization (FCM) shows a fairly sharp, positive increase below 336 K which remains essentially a constant value above the ZFCM at lower temperatures as shown in Fig. 4-1. Although this magnetic behavior is uncharacteristic for a bulk superconductor at its transition temperature, we have observed resistive drops in the same temperature range in other ceramic YBaCuO samples and nominal $YBa_2Cu_3O_{7-\delta}$ single samples. (See preceding two sections.) Furthermore, one of the earliest reports of zero-resistance transitions above room temperature was at 340 K in a $YBaSrCu_3O_7$ sample reported by a Japanese group.[2] The strong coincidence in the 340-K temperature between these various superconducting-like results suggested a more thorough study should be pursued. We have correspondingly pursued a three prong attack to this problem. (i) We have systematically studied the synthesis conditions for growing samples which exhibit this 336-K transition by utilizing our simultaneous differential thermal analyzer and thermogravimetry (DTA/TG) system. (ii) Subsequently we have utilized x-ray diffraction (XRD) and electron microscopy to assist in the identification of possible crystal phases and/or structural feature that could be associated with the appearance of the 336-K transition. (iii) In addition, we have tried to characterize the nature of this transition more fully and its possible relation to surface superconductivity. During the past 36 months, over one hundred-fifty ceramic YBaCuO samples were tested for the possible existence of the 336-K transition by low-field magnetization measurements, with nearly 50% exhibiting some indication of this unusual magnetic behavior.

The first phase of this research was to repeat the synthesis conditions utilized in the previous preparation of nominal $Y_5Ba_6Cu_{11}O_y$ samples exhibiting this 336-K magnetic transition. Five different batches of 5:6:11 (Y:Ba:Cu) nitrate and oxide powders were mixed and homogenized in a nitric acid solution. After heating to 950°C in flowing O_2 for 18 hours, the reacted powders were quenched to room temperature in air. This procedure was repeated four more times with intermediate grindings. Out of the five batches, samples from only two batches clearly exhibited the characteristic magnetic behavior at 336 K. (See Fig. 4-1 for the magnetic characteristics for a sample from these batches.) Even though the

synthesis conditions were the same, the lack of total reproducible results indicated a more systematic and informative approach to the synthesis procedure, such as afforded by the DTA/TG system, would be beneficial. This was especially true since a knowledge of the reaction processes during the cooling cycle could be easily monitored.

Utilization of the DTA/TG system in the sample synthesis permitted the variation of several parameters including the relative O_2 partial pressure, the inert gas to be utilized, different final heating temperatures, different hold times at the highest temperatures. Also variations in the relative Y:Ba:Cu compositions as well as in starting materials were tested. (See Table I.) The following summarizes our findings of the synthesis conditions for increased probability of growing samples which will exhibit the 336-K magnetic transition.

(1) Heating in a pure Ar gas flow rather than in He or N_2 gas flow.

(2) Minimizing the O_2 present from the outgassing of unreacted samples.

(3) Presence of a sharp solidification peak in the DTA data during the cooling cycle is beneficial, but not absolutely necessary. (See Fig. 4-2.)

(4) Disappearance of 336-K magnetic transition dependent upon annealing time, temperature, and gas. The FCM becomes coincident with the ZFCM after a long-time (24 hr) anneal in O_2 at 500°C - 600°C. The 336-K transition reappears in the sample after a subsequent 800°C Ar anneal.

(5) Starting compositions or materials play a secondary role in the formation of samples exhibiting the 336-K transition as long as excess CuO is present.

Table I. DTA/TG Synthesized Samples

Nominal Composition (Y:Ba:Cu)	Starting Materials	336-K Transition Present
1 : 2 : 2.75	nitrates & oxides powders & HNO_3	yes
1 : 2 : 3	$YBa_2Cu_3O_7$	no
1 : 2 : 4	$YBa_2Cu_3O_7$ & CuO	no
1 : 2 : 4	$YBa_2Cu_4O_8$ (trace $BaCuO_2$)	yes
1 : 2 : 4	nitrates & oxides ($Y_{0.8}Ca_{0.2}SrBaCu_4O$)	no
4 : 5 : 9	$YBa_2Cu_4O_8$ & Y_2BaCuO_5	yes
4 : 5 : 9	carbonates	yes
4 : 5 : 9	nitrates & oxide powders & HNO_3	yes
2 : 2 : 4	carbonates	yes
1 : 3 : 5	nitrates & oxide powders & HNO_3	yes

Also since the majority of these samples were grown in flowing Ar and not pressed into pellets, the samples are highly resistive, or even insulating, and thus electrical measurements are not available.

Depending upon the final heating temperature, a maximum of six different reactions can be observed during the heating cycle in samples containing Y:Ba:Cu ratios of 1:2:4 and 4:5:9. (See Figs. 4.3 - 4.4.) These include the decomposition of $YBa_2Cu_4O_8$ into the 123 phase and CuO, the e1* and e2 eutectic reactions, the p1 and p2 peritectic reactions, and the c3 melting reaction with the corresponding reaction temperatures decreasing with decreasing oxygen partial pressure. All of these reactions have been previously described in the literature[3,4] except for the e1* eutectic reaction. The temperature of this reaction is consistently higher than the reported e1 eutectic associated with the 123 phase reacting with $BaCuO_2$ and CuO to form a liquid phase. Instead, the e1* eutectic appears to be the result of the 124 phase or the intermediate $Y_2Ba_4Cu_7O_{15}$ (247) phase reacting with $BaCuO_2$ and CuO and forming a liquid melt. Since the 124 phase can transform into the 247 phase and CuO before decomposing into the final products of 123 phase and CuO, we cannot distinguish which is the more appropriate reactant. The identification of the e1* reaction has gained added importance since a couple of DTA/TG measurements on 1:2:4 samples indicated that the heating temperature had only to exceed this e1* reaction temperature in order for samples to exhibit the 336-K magnetic transition and not necessarily the eutectic e2 or peritectic p2 reaction temperatures. The determination of which of these two reactions - e1* or e2/p2 - is more important, is still uncertain because of the close proximity in their respective reaction temperatures and the overlap of their respective broad endothermic peaks.

Structural and surface studies by XRD and SEM are presently unable to provide a clear indication of the phase associated with the 336-K transition in these multi-phase samples. XRD data indicate a few common features present in those samples exhibiting the 336-K transition. First, the predominate phases in most samples are the nonsuperconducting tetragonal $YBa_2Cu_3O_{6.0}$ and the insulating Y_2BaCuO_5 structures with smaller amounts of insulating Cu_2O and $BaCu_2O_2$. However two sets of peaks associated with the tetragonal 1-2-3 phase are anomalous: the intensities of the (103)/(013) and (110) peaks are nearly equal in magnitude although the ratio should be closer to 2:1; and the relative intensities for the (003) and (100)/(010) do not agree the literature values. (See Fig. 4-5 to 4-7.) This

suggests a possible distortion of the lattice or chemical substitution for certain atoms in these particular planes. Also it should be pointed out that magnetization data below 100 K show a clear diamagnetic response below 60 K, indicating the presence of the superconducting $YBa_2Cu_3O_{6.5}$ phase. Since this phase is not observed in the XRD patterns, this phase represents less than 2% of the sample or possibly exists as a thin surface layer. Furthermore since the maximum temperatures during the DTA/TG synthesis of many samples exceeded the peritectic melting temperature, these samples have some melting occurring which is supported by the SEM topographical studies.

These most recent DTA/TG findings in conjunction with the XRD data have lead us to speculate that the 124 or 247 phase decomposes in an Ar environment at e1* into another oxygen-deficient, non-123 Y-Ba-Cu-O phase and is responsible for the magnetic phenomenon. The formation of this phase is extremely slow and is more easily detected in the DTA/TG measurements by the recrystallization process from the Ba-Cu-rich liquid melt as indicated by the appearance of an exothermic peak in the cooling curves near 850°C when 1:2:4 and 4:5:9 samples have been heated above the e2 and p2 reaction temperatures. The identification of this non-123 phase has not been successful to date because the sluggishness of its formation during the cooling prevents sufficient quantities from being formed and subsequently detected by normal XRD measurements. Furthermore, the oxygen stoichiometry of this phase is critical as a small oxygen partial pressure (10^{-3} bar) is sufficient to prevent the formation of the correct oxygen-deficient YBaCuO phase responsible for the 336-K magnetic transition. Nevertheless, this latter feature has provided some insight into the nature and origin of the magnetic hysteresis.

The last aspect of this research is the study of the nature of this 336-K transition. An investigation of the magnetic field dependence of the FCM showed the abrupt, positive increase below 336 K to be essentially field independent for fields from 0.5 to 1000 Oe. On the other hand, the ZFCM began to exhibit an increase just below 336 K for fields above 10 Oe as shown in Figs. 4-8 to 4-10. This behavior is reproducible as measurements repeated many times on a given sample resulted in the same ZFCM and FCM within the sensitivity of the SQUID magnetometer. Some of the measurements were performed after the sample had been placed in a desiccator for two years. In addition, the change in the sample orientation and after pulverization of a sample had no effect on the observed magnetic behavior nor the 336-K transition temperature.

These features at 336 K can be best understood in terms of the realignment of the moments of a canted antiferromagnet where the moments in the field-cooled measurements would realign along the field direction giving rise to an enhanced, ferromagnetic-like component in the magnetization. This type of canted antiferromagnetism or weak ferromagnetism has been previously reported in the La_2CuO_4 T-structure and Nd_2CuO_4 T'-structure.[5-7] A slight deviation from the perfect tetragonal symmetry of these crystal structures gives rise to antisymmetric exchange interaction, known as the Dzyaloshinsky-Moriya (DM) interaction,[8,9] between the Cu moments which causes a canting of the Cu moments away from a strictly antiferromagnetic alignment. In the presence of a magnetic field, the canted Cu moments line up in the direction of the applied field and produce a weak net magnetization of the Cu moments. This gives the appearance of a spontaneous ferromagnetic-like transition in the FCM curves. The deviations that give rise to the DM interaction and eventual weak ferromagnetism may be in the form of temperature-dependent structural changes resulting from lattice defects and variance in the oxygen stoichiometry. This type of scenario is consistent with the presence of a small amount of an antiferromagnetic, oxygen-deficient YBaCuO phase being responsible for the 336-K magnetic transition. However, until sufficient quantities of this material phase are synthesized, there will remain some question as to the exact nature of the 336-K magnetic transition as well as the identification of the material phase itself.

5. *STUDIES OF THE PARAMAGNETIC MEISSNER EFFECT*

The paramagnetic Meissner effect (PME) or Wohlleben effect is a characteristic property of certain superconducting samples whose field-cooled-magnetizations (FCM) are positive below their superconducting transition temperature T_c, instead of the usual diamagnetic behavior associated with the Meissner effect. The first reports of this PME behavior were on certain melt-cast BiSrCaCuO samples[10,11] in which the FCM/H became increasingly positive with decreasing magnetic fields suggesting that spontaneous currents would be set up in the limit of zero field. This unusual magnetic phenomenon naturally led to several speculations as to its origins, including spontaneous orbital currents arising from π-junctions formed at superconducting grain boundaries.[12] These spontaneous currents could occur as the result of the π-phase shift in the tunneling process between two *d*-wave superconductors joined at different crystallographic orientations.[13] Consequently the observation of the PME has been cited in numerous papers as supporting evidence for *d*-

wave superconductivity in the cuprate superconductors. Thus there has been great interest in further elucidating the nature of this effect and its origin. In previous annual technical report, we presented results of a similar observation of a paramagnetic Meissner effect in Nb disks. Our work[14] clearly points out that the PME is not unique to the high-T_c superconductors and probably not related to the symmetry of the superconducting order parameter since Nb is a conventional *s*-wave superconductor. In this report, we provide additional details of the magnetic and material characteristics of the Nb disks that exhibit the PME.

The diamagnetic shielding and flux expulsion for nearly two dozen Nb disks have been studied as a function of temperature and magnetic field. Figure 5-1 displays the low-field dependence of both the zero-field-cooled magnetization (ZFCM) and the FCM for fields applied perpendicular to the surface of a typical (untreated) 0.127-mm thick Nb disk. At the lowest temperatures, the ZFCM/H shows complete shielding with the magnitude of the diamagnetic signal being approximately 22 times larger than $-V/4\pi$ due to the local field enhancement arising from the geometric demagnetization factor for this disk-field orientation. With increasing temperature, the ZFCM data indicate the presence of two major diamagnetic transitions at 9.06 K and 9.2 K, the latter being strongly field-dependent. This strong field-dependent behavior in conjunction with the large decrease in the magnitude of the ZFCM/H suggest that the local field at the disk's edge exceeds the lower critical field $H_{c1}(T)$ in the temperature range above 9.06 K. The appearance of two transitions is also apparent in the field-cooled measurements with decreasing temperature. Initially the FCM shows a weak diamagnetic response below 9.26 K, followed by an abrupt increase in the FCM at 9.20 K which continues to increase until at 9.06 K where the FCM becomes essentially constant. One should also note that the temperature associated with the abrupt FCM increase is identical to the temperature where the large diamagnetic response in the ZFCM data becomes nearly zero. In fact, the temperatures associated with these two features remain correlated for other samples even though the features can occur at various temperatures between 9.08 K and 9.24 K depending upon different sample treatments. It should be further noted that the appearance of the shoulder in the ZFCM occurs in all of our Nb disks exhibiting the PME as well as those reported by the Argonne group.[15] This indicates that a material characteristic associated with the observation of the PME is that these Nb disk samples are inhomogeneous superconductors with variations

in their T_c. This characteristic of inhomogeneous superconductivity was even evident in some of the earliest PME work[11] on the BiSrCaCuO samples.

Another unusual characteristic associated with the PME in the Nb disks is the nearly "ideal" Bean model-like hysteresis curves in the temperature range of the ZFCM shoulder of 9.05 to 9.15 K as shown in Fig. 5-2. After an initial linear rise in the magnetization due to the edge screening currents maintaining complete flux exclusion, the magnetization becomes nearly field-independent indicating a large resistance to the movement of magnetic vortices into the sample. This large viscosity is further evidenced by the reversal of the screening current direction upon a decrease in the magnetic field after reaching the maximum field strength of 5 Oe. The origin for the very viscous nature of the vortices is unclear at this time, but it is reasonable to speculate from the surface morphology that the cold-rolled process has created numerous voids and serrations which act as effective pinning sites. Perhaps the interaction between the screening currents and the flux being trapped near the circumferential edges is sufficient to prevent further vortex movement into the disks.

Another magnetic feature of the Nb disk samples is that only diamagnetic responses are observed for both the ZFCM and FCM when fields are applied parallel to the disk surfaces. (See Fig. 5-3.) With increasing temperatures, the parallel-field data show a large diamagnetic transition at about 9.06 K with the remaining 10% of the signal showing a more gradually decrease until it vanishes at 9.26 K. Also the field dependences at all temperatures are extremely weak. This anisotropic behavior indicates a preferred orientation of the sample with respect to the magnetic field direction in order to observe the PME, i.e., the field should be perpendicular to the largest geometric dimensions. This observation is also consistent with the recent observation of the PME on YBaCuO single crystal samples.[16]

The occurrence of the PME is also predicated on the surface microstructure. As previously reported,[14] altering the surface by mechanical abrasion, oxygen annealing, and chemical etching can have a profound effect on the PME, including its elimination. Figure 5-4 demonstrates the reduction and eventual elimination of the PME as well as of the shoulder in the ZFCM data through a sequence of mechanical sanding of both the top and bottom disk surfaces. For this particular disk, the removal of about 5 μm from both surfaces was sufficient for the PME to completely disappear. In addition to the disappearance of the PME, the ZFCM data show a singular diamagnetic transition which

has shifted to higher temperatures even though less than 10% of the total sample volume was removed. This points out that surface microstructure not only plays a significant role in the PME formation but also affects the ZFCM which often is thought to represent the "bulk" nature of the superconducting sample's volume and temperature.

Further evidence that the surface microstructure is crucial to the occurrence of the PME is found in the following set of experiments. Nb disks of 0.25-mm thickness, which have a similar surface morphology as the thinner 0.127-mm thick disks, do not exhibit the PME as seen in Fig. 5-5. After implanting both sides of a 0.25-mm thick Nb sheet with 200 keV Kr ions at 6 x 10^{16} dose/ cm^2, disks punched from the implanted sheet exhibited ZFCM and FCM for perpendicular fields strikingly similar to those of the thinner Nb disks exhibiting the PME. (See Fig. 5-5.) These results include the appearance of a positive FCM/H response below 9.17 K which increases with decreasing fields and the shoulder in the ZFCM data above 9.07 K with its strong field dependence. Furthermore, only diamagnetic ZFCM and FCM responses were observed in the parallel orientations for the ion-implanted disks while the PME characteristic behavior vanished after mechanical abrasion of both surfaces. The penetration of the Kr ions into the Nb disk is restricted to about the first 100 nm below the surface. This relatively shallow penetration is sufficient to induce the PME by creating a variation in the T_c near the disk surface as well as leading to defect structures for enhanced flux pinning. In contrast, thinner Nb disks (t=0.025 mm) did not exhibit the PME either before or after identical ion implantation. Hence it is not simply a matter of the Kr ions introducing a paramagnetic moment by virtue of their presence in the sample. Rather, the surface microstructure plays the key role in the appearance of the PME in these Nb disks and must be related to the geometric dimensions of the sample. Due to the preferred perpendicular field orientation for observing the PME, the thickness of the disks compared to the depths of the surface microstructural features is the most probable dimension to be considered.

Our investigations suggest the PME arises from inhomogeneous local field distributions resulting from the sample geometry and microstructural surface features including variations in the T_c and the presence of strong pinning sites. Furthermore, the PME in these Nb disks is neither an intrinsic superconducting property of Nb nor related to the symmetry of its superconducting pairing mechanism.

6.STUDIES OF JOSEPHSON EFFECTS IN OXIDE SUPERCONDUCTORS

It is generally believed that the superconductivity in the high-T_c cuprates is intrinsically two-dimensional residing in the CuO_2 bilayers or trilayers coupled together by the Josephson currents along the *c* -axis direction. Theories and experiments involving several phenomena and properties, including angular dependence of the critical current, upper critical field, and far-infrared conductivity all support this picture. Recently Kleiner, *et al.* [17,18] have shown that the current-voltage (I-V) characteristics of a single crystal of $Bi_2Sr_2CaCu_2O_{8+\delta}$ (BSCCO) as well as that of other high-T_c cuprates consisted of numerous branches indicative of a stack of Josephson tunnel junctions. According to the magnetic-field periods derived from the magnetic-field dependences of the critical current, the Josephson junctions are formed by the inter-unit-cell CuO_2 bilayers. However, a search for similar Josephson-junction-like I-V characteristics in $YBa_2Cu_3O_{7-\delta}$ (YBCO) was unsuccessful. This raised a question whether the superconductivity in YBCO was bulk-like as opposed to a stack of Josephson junctions as in BSCCO. Recently we have found experimental evidence not only for the existence of inter-unit-cell Josephson junctions in YBCO but also intra-unit-cell Josephson junctions formed by the CuO_2-Y-CuO_2 atomic planes.[19]

By measuring the dynamic resistance dv/di of a YBCO single crystal near T_c as a function of the magnetic field H, two groups of peak structures with nearly uniform magnetic field spacings are observed. Figure 6-1 shows two peaks, one centered at 90 G and the other close to 220 G. Utilizing the magnetic flux quantization condition for a thin electrode Josephson junction and the geometric dimensions of the YBCO crystal, the spacing between electrodes was calculated to be 0.34 ± 0.09 nm which is in good agreement with the separation between the CuO_2-Y-CuO_2 atomic planes of 0.32 nm. At a slightly lower temperature, the dynamic resistance (see Fig. 6-2) shows many more resistive peaks with smaller magnetic field spacings. Upon careful inspection of this and other data, these results suggest two group of peaks with different spacings of $\Delta H \sim 30$ G and 15 G. The thickness associated with these magnetic spacings would be 1.1 nm and 2.1 nm, the former corresponding to the separation of the CuO_2 bilayers between the different unit cells. We have also observed evidence that the intrinsic Josephson junctions in a YBCO single crystal evolve naturally from the short-junction into the long-junction regime as the temperature is reduced. Since these findings of an intra-unit-cell Josephson junction in YBCO have a strong implication for the occurrence of atomic-plane 2-D

superconductivity in the cuprate superconductors, we are continuing these investigations to further elucidate the nature of the Josephson effects in the cuprate superconductors.

In a second investigation, we have studied the effects of microwave radiation on YBCO single crystals to see the effect of the intrinsic Josephson junctions. By placing a single crystal in an X-band waveguide which has well-behaved microwave E- and H-fields, we have systematically studied the roles of the microwave E- and H-fields in determining the dynamic properties of a YBCO single crystal. Microwave induced dc voltages in a $YBa_2Cu_3O_{7-\delta}$ single crystal have been observed along its *c* -axis with or without a dc bias current by utilizing standing waves near the end of an X-band (8-12 GHz) waveguide. With a dc bias current, the effect is larger when the single crystal is coupled to the maximum of the microwave H-field, suggesting that the induced dc voltages are due to vortex flow. (See Fig. 6-3.) Without a dc bias current, the induced voltages resemble the inverse ac Josephson effect and require the presence of both the E- and H-fields of the microwave. The temperature and the bias current dependences of the induced voltages both show several peak structures indicating the existence of multiple Josephson junctions in series along the *c* -axis direction of the single crystals. However, it is not yet clear whether the Josephson junctions are formed within a unit cell or at the stacking faults which commonly occur in a single crystal sample.

Further support for this Josephson junction hypothesis comes from our observation of periodic voltage oscillations as a function of magnetic field when a dc bias current is applied along the *c* -axis of a $YBa_2Cu_3O_{7-\delta}$ single crystal and the dc magnetic field is applied parallel to the *ab* -planes of the crystal. The voltage-vs-field patterns are similar to the magnetic interference patterns associated with a dc SQUID. Studies to further elucidate these features as well as to improve our understanding of these effects in the cuprate superconductors are still continuing.

7. REFERENCES

1. J.T. Chen, L-X. Qian, L-Q. Wang, L.E. Wenger, and E.M. Logothetis, *Modn. Phys. Lett B* 3, 1197 (1989); in *Superconductivity and Applications*, edited by H.S. Kwok, Y-H Kao, and D.T. Shaw, (Plenum, New York, 1989), pp. 517-529.

2. H. Ihara, N. Terada, M. Jo, M. Hirabayashi, M. Tokumoto, Y. Kimura, T. Matsubara, and R. Sugise, *Jpn. J. Appl. Phys.* **26**, L1413 (1987).

3. T. Aselage and K. Keefer, J. Mater. Res. **3**, 1279 (1988).

4. K.W. Lay and G.M. Renlund, J. Amer. Cer. Soc. **73**, 1208 (1990).

5. S.B. Oseroff, D. Rao, F. Wright, D.C. Vier, S. Schultz, J.D. Thompson, Z. Fisk, S.W. Cheong, and M.F. Hundley, Phys. Rev. B **41**, 1934 (1990).

6. M. Tovar, X. Obradors, F. Perez, S.B. Oseroff, R.J. Duro, J. Rivas, D. Chateigner, P. Bordet, and J. Chenevas, Phys. Rev. B **45**, 4279 (1992).

7. M. Bennahmias, H.B. Radousky, C.M. Buford, A.B. Kebede, M. McIntyre, T.J. Goodwin, and R.N. Shelton, Phys. Rev. B **53**, 2773 (1996).

8. J. Dzyaloshinsky, J. Phys. Chem. Solids **4**, 241 (1958).

9. T. Moriya, Phys. Rev. **120**, 91 (1960).

10. P. Svedlindh, K. Niskanen, P. Norling, P. Nordblad, L. Lundgren, B. Lönnberg and T. Lundström, Physica C **162-164**, 1365 (1989).

11. W. Braunisch, N. Knauf, G. Bauer, A. Kock, A. Becker, B. Freitag, A. Grütz, V. Kataev, S. Neuhausen, B. Roden, D. Khomskii, D. Wohlleben, J. Bock, and E. Preisler, Phys. Rev. B **48**, 4030 (1993).

12. D. Khomskii, J. Low Temp. Phys. **95**, 205 (1994).

13. M. Sigrist and T.M. Rice, Rev. Mod. Phys. **67**, 503 (1995).

14. D.J. Thompson, M.S.M. Minhaj, L.E. Wenger, and J.T. Chen, Phys. Rev. Lett. **75**, 529 (1995).

15. P. Kostic, B. Veal, A.P. Paulikas, U. Welp, V.R. Todt, C. Gu, U. Geiser, J.M. Williams, K.D. Carlson, and R.A. Klemm, Phys. Rev. B **53**, 791 (1996).

16. S. Riedling, G. Bräuchle, R. Lucht, K. Röhberg, H. v. Löhneysen, H. Claus, A. Erb, and G. Müller-Vogt, Phys. Rev. B **49**, 13283 (1994).

17. R. Kleiner, F. Steinmeyer, G. Kunkel, and P. Müller, Phys. Rev. Lett. **68**, 2394 (1992); R. Kleiner and P. Müller, Phys. Rev. B **49**, 1327 (1994).

18. R. Kleiner, P. Müller, H. Kohlstedt, N.F. Pedersen, and S.Sakai, Phys. Rev. B **50**, 3942 (1994).

19. D.C. Ling, J.T. Chen, Grace Yong, and L.E. Wenger, Phys. Rev. Lett. **75**, 2011 (1995).

LIST OF FIGURES

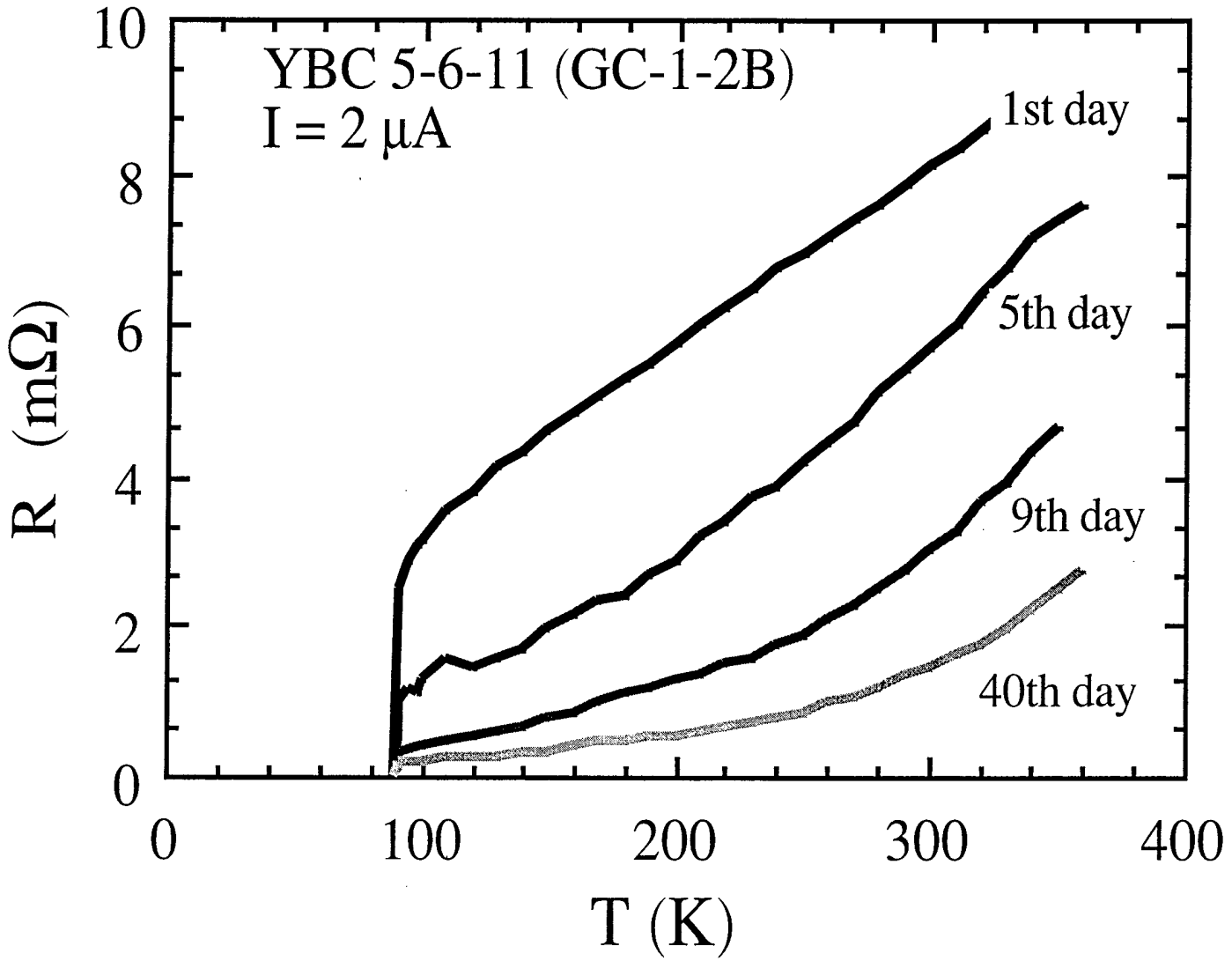

Fig. 2-1. The time dependence of the resistance for a nominal 5:6:11 YBaCuO multi-phase ceramic sample in 2 atm of O_2 gas as a function of temperature.

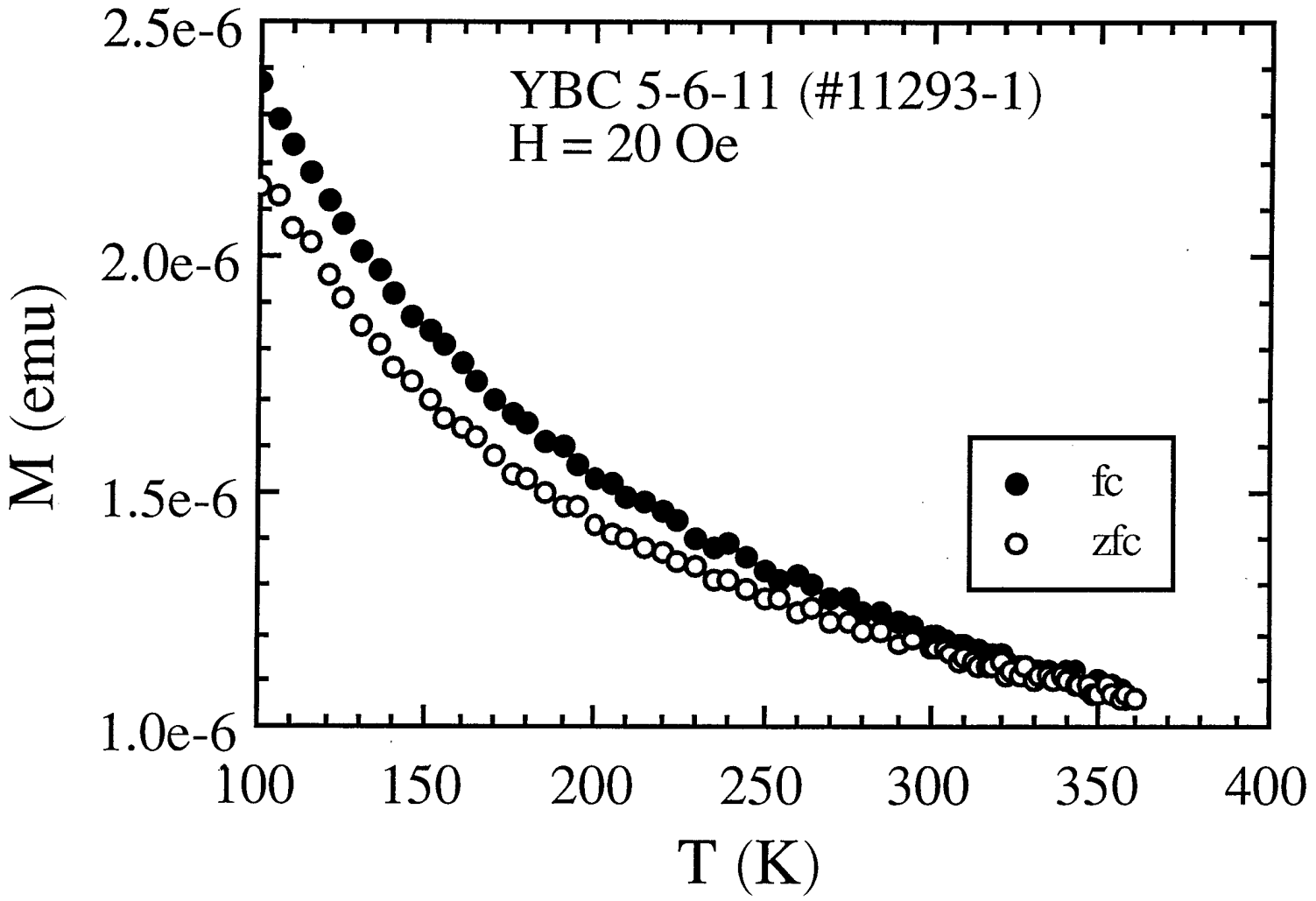

Fig. 2-2. The ZFCM and FCM for a multi-phase YBaCuO sample of nominal composition 5:6:11. Note the ZFCM continuously deviates from the FCM below 320 K.

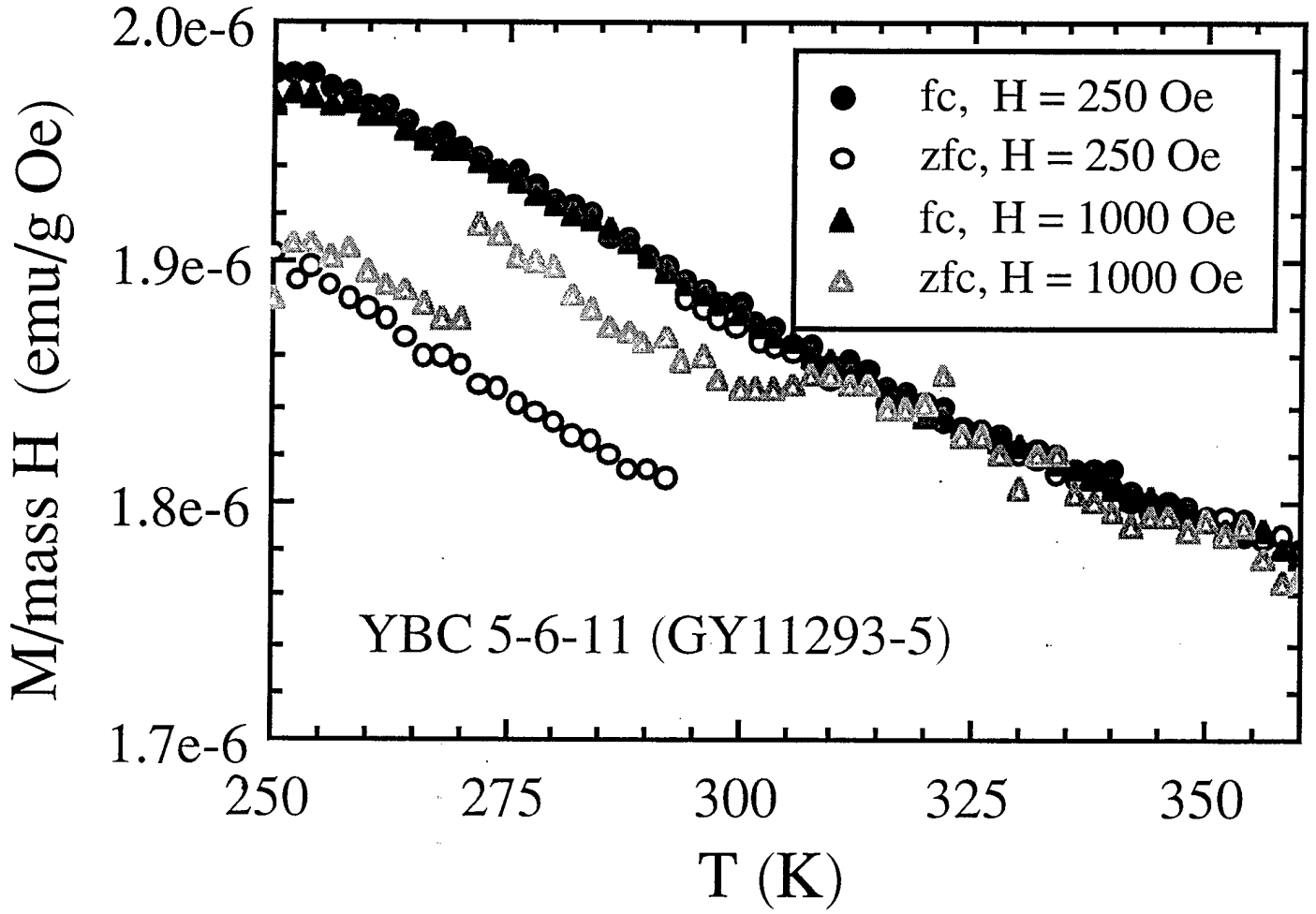

Fig. 2-3. The ZFCM and FCM for a ceramic 5:6:11 YBaCuO sample for two different fields, 250 Oe and 1000 Oe. Note that the flux jumps as well as the diamagnetic-like deviations at 310 K.

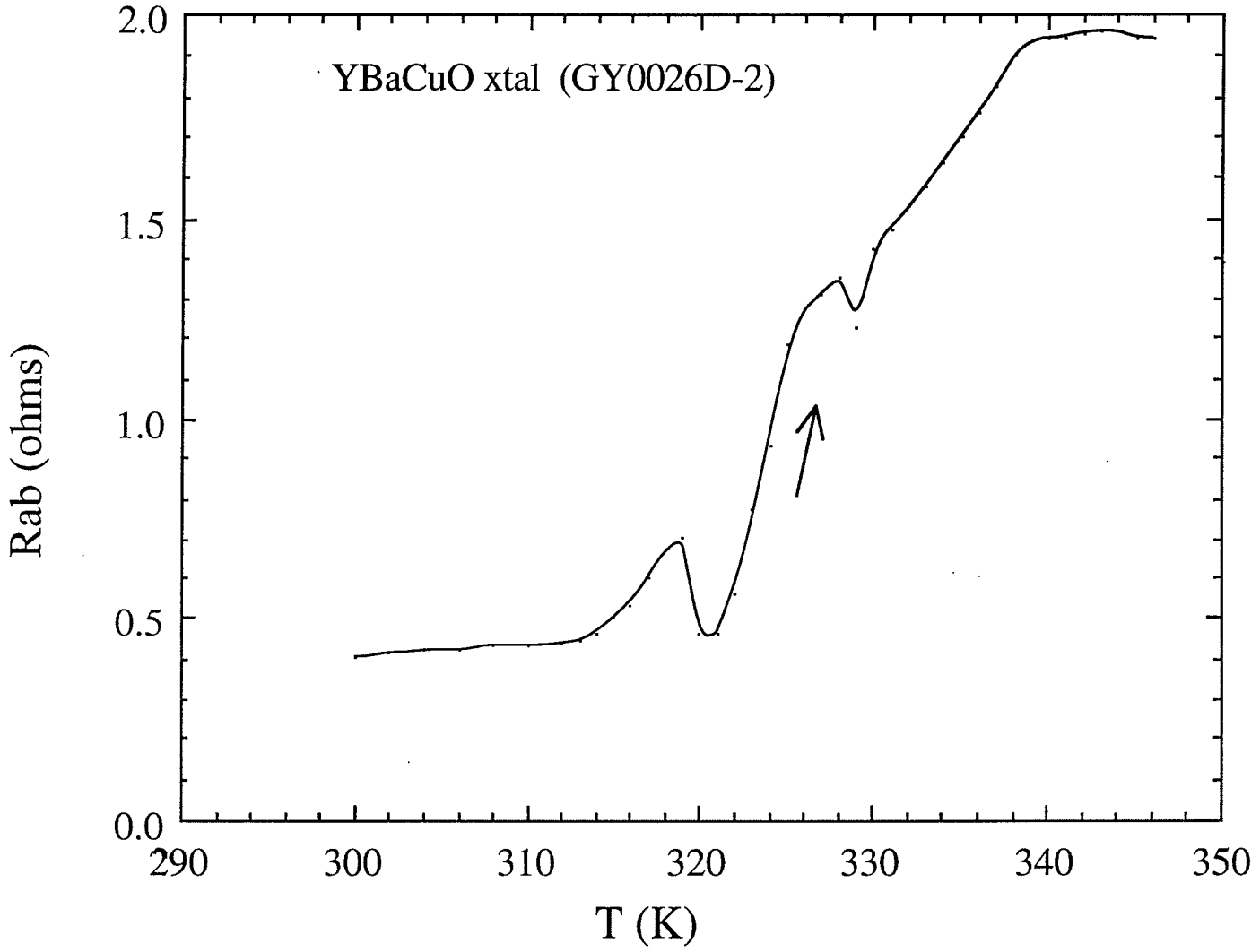

Fig. 3-1. Resistance along *ab*-plane of a nominal $YBa_2Cu_3O_{7-\delta}$ single crystal showing a resistive transition in the vicinity of 340 K.

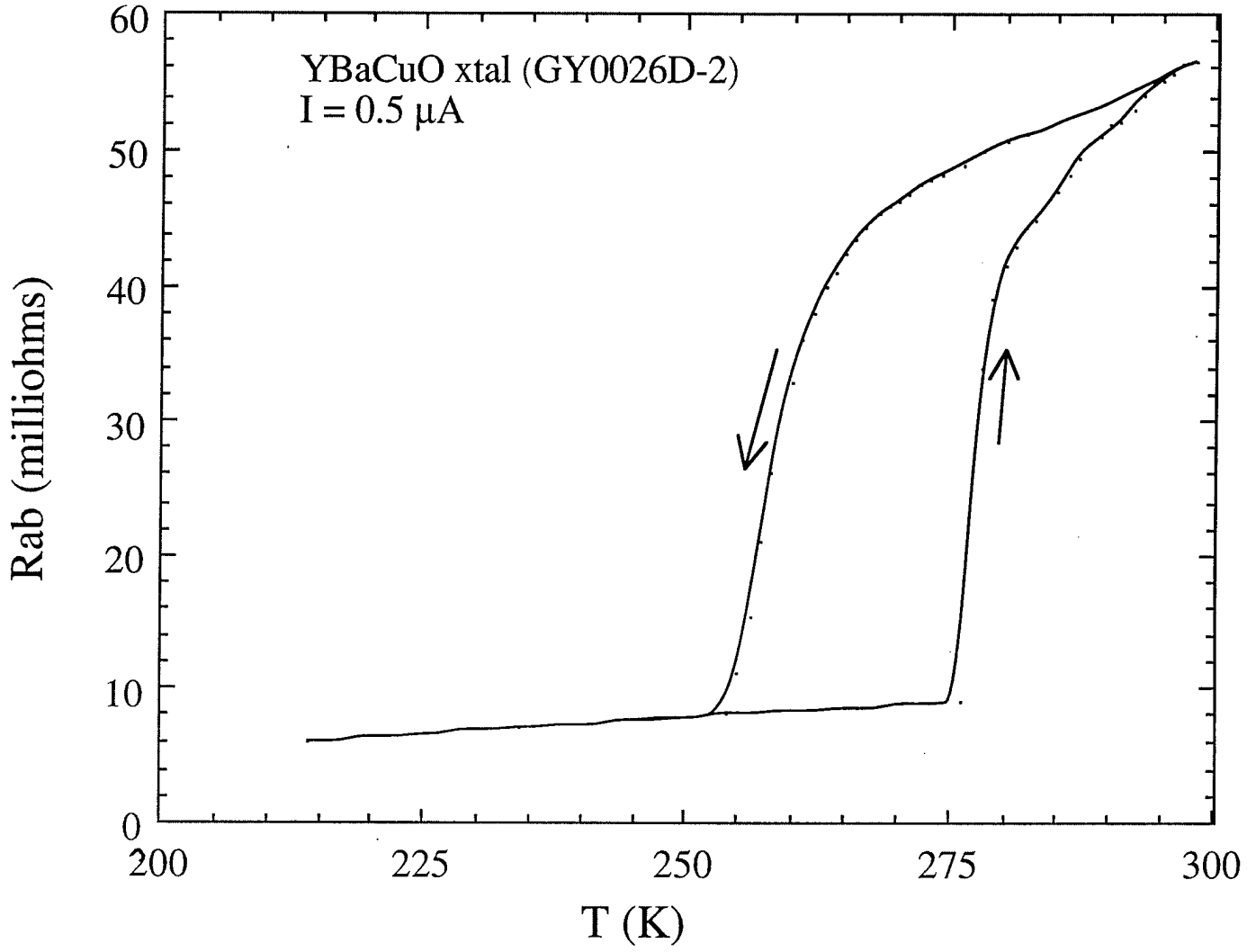

Fig. 3-2. Resistance along *ab*-plane of a nominal $YBa_2Cu_3O_{7-\delta}$ single crystal showing a hysteretic behavior in the resistive transition below 280 K.

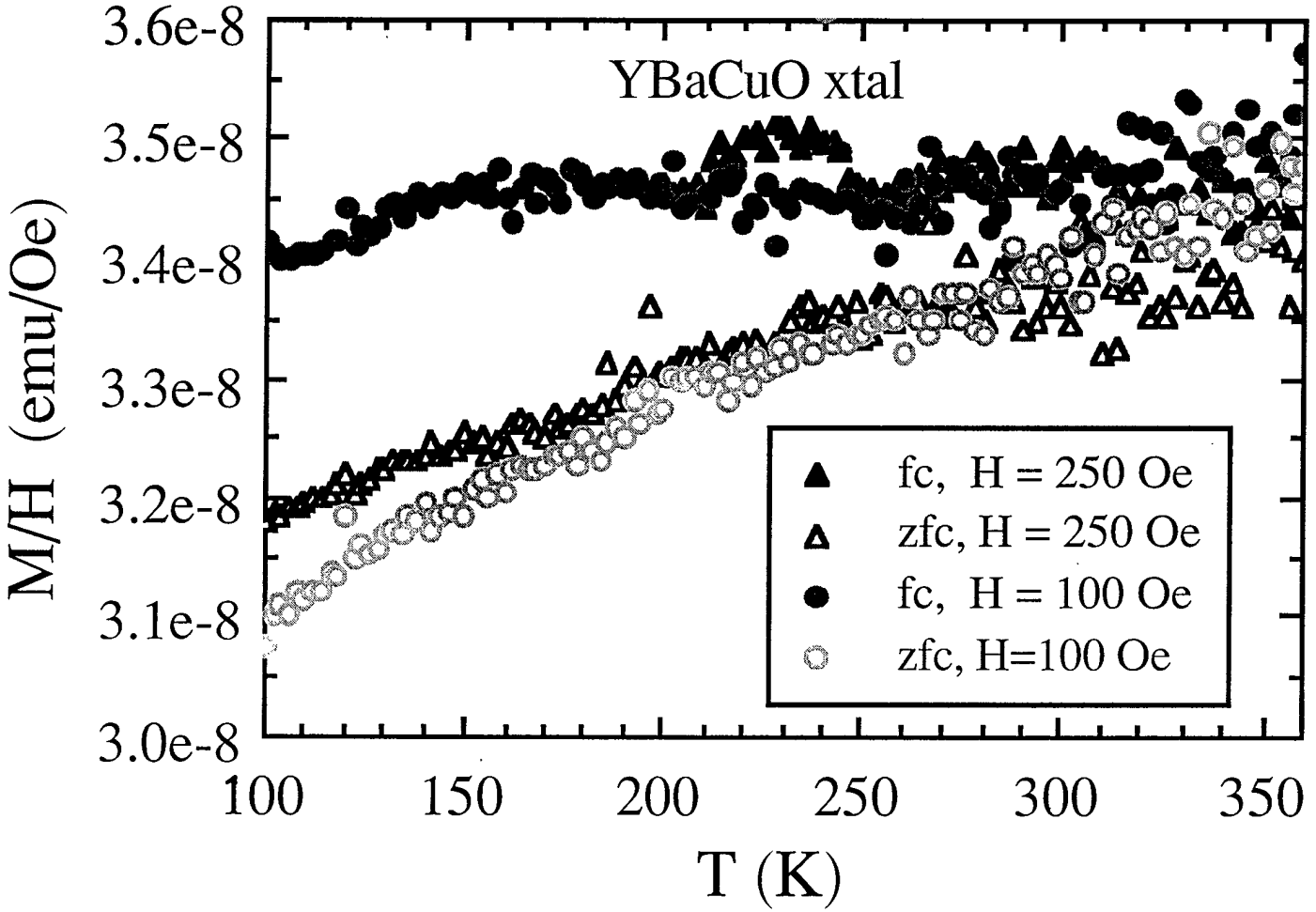

Fig. 3-3. The ZFCM and FCM for a nominal $YBa_2Cu_3O_{7-\delta}$ single crystal sample (91093-4) in fields of 100 Oe and 250 Oe.

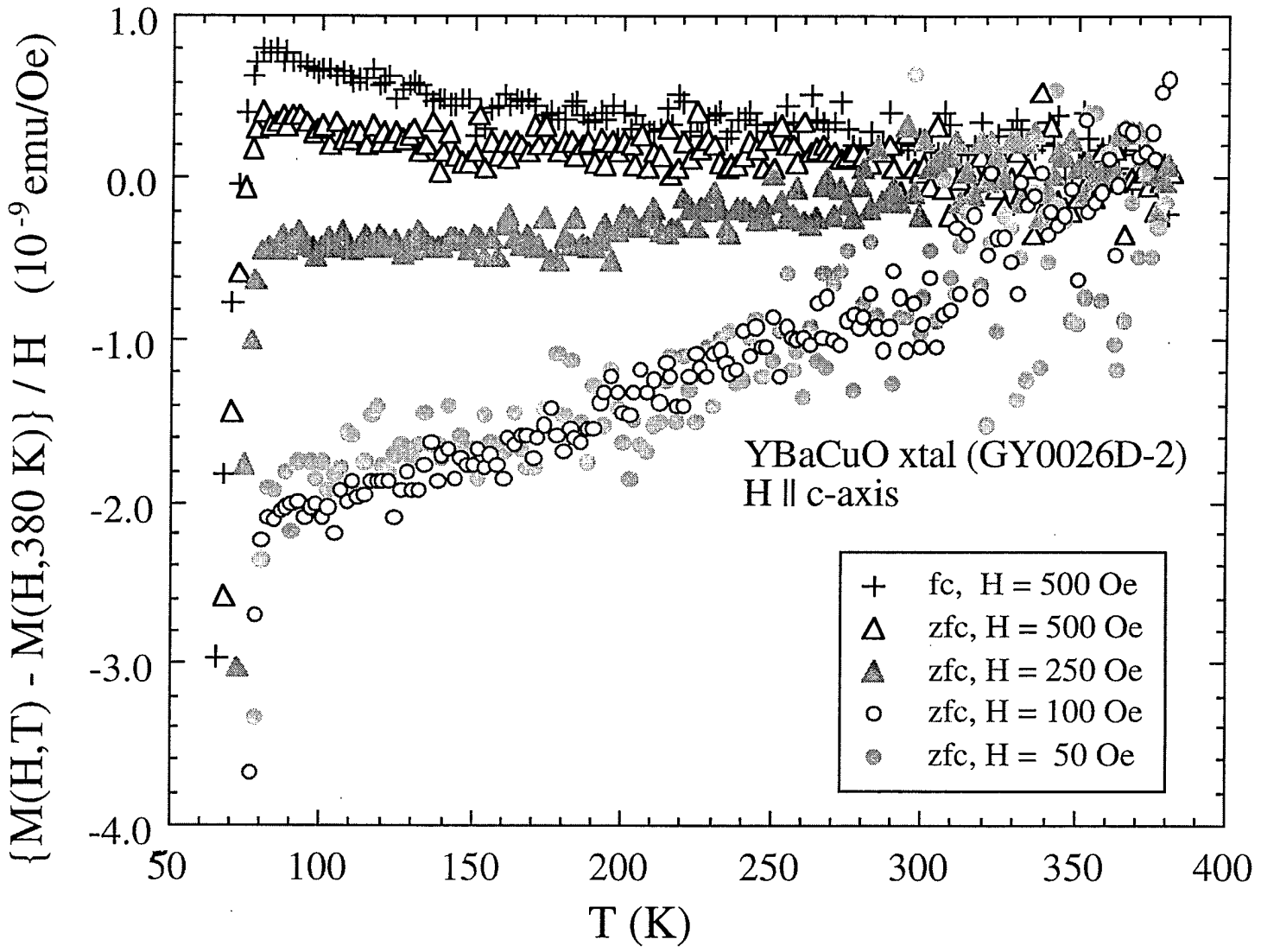

Fig. 3-4. The ZFCM and FCM for a nominal $YBa_2Cu_3O_{7-\delta}$ single crystal sample (GY0026D-2) exhibiting a 340 K resistive transition. Note that the hysteretic behavior begins at 340 K and the ZFCM/H approaches the FCM/H data for fields larger than 100 Oe.

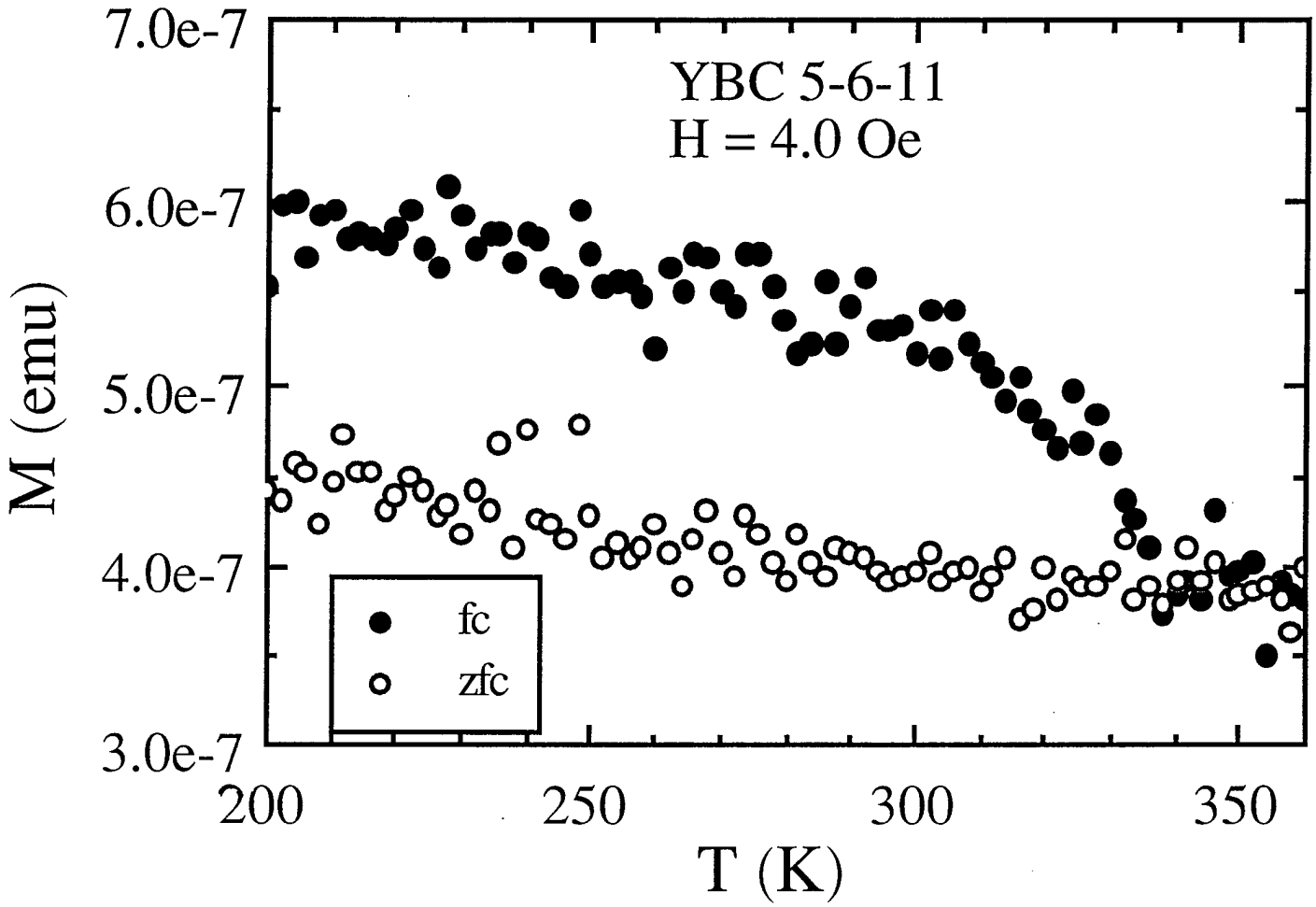

Fig. 4-1. The ZFCM and FCM for a nominal 5:6:11 YBaCuO sample which exhibits a 336-K transition.

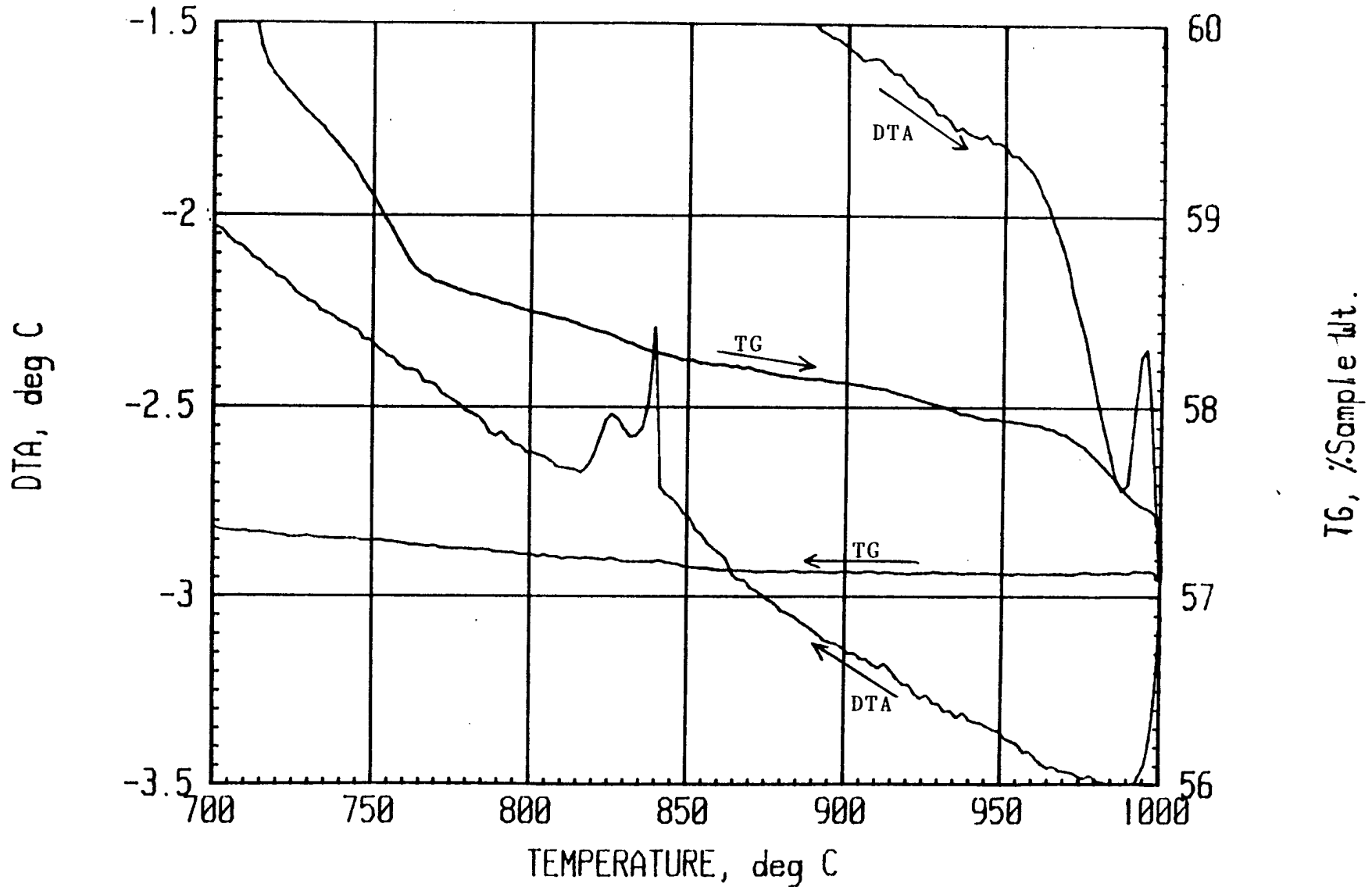

Fig. 4-2. Simultaneous DTA/TG data during the warming and cooling cycles of the synthesis of a nominal 1 : 2 : 2.75 YBaCuO sample in Ar gas.

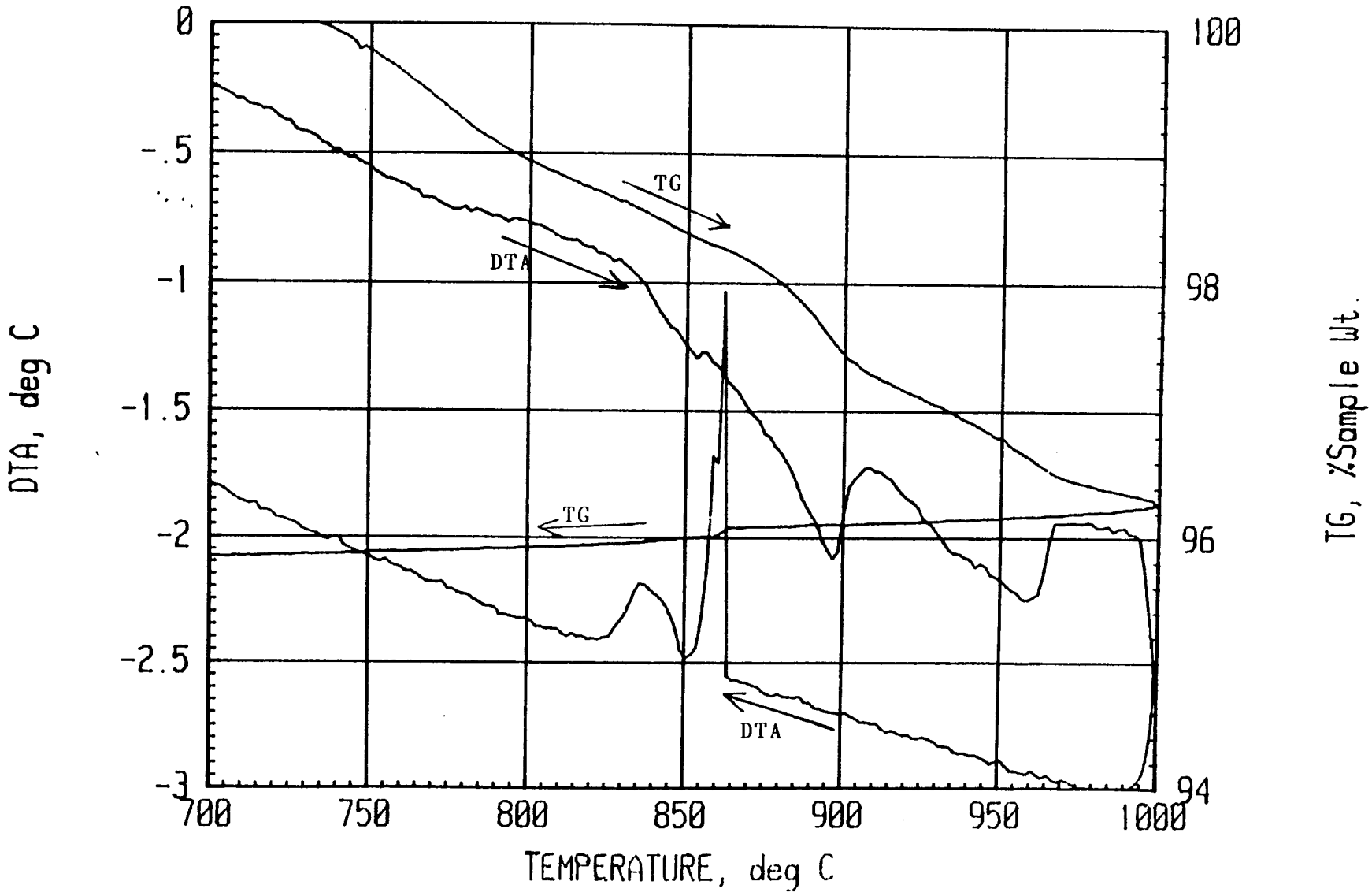

Fig. 4-3. Simultaneous DTA/TG data during the warming and cooling cycles of the synthesis of a nominal 1 : 2 : 4 YBaCuO sample in Ar gas.

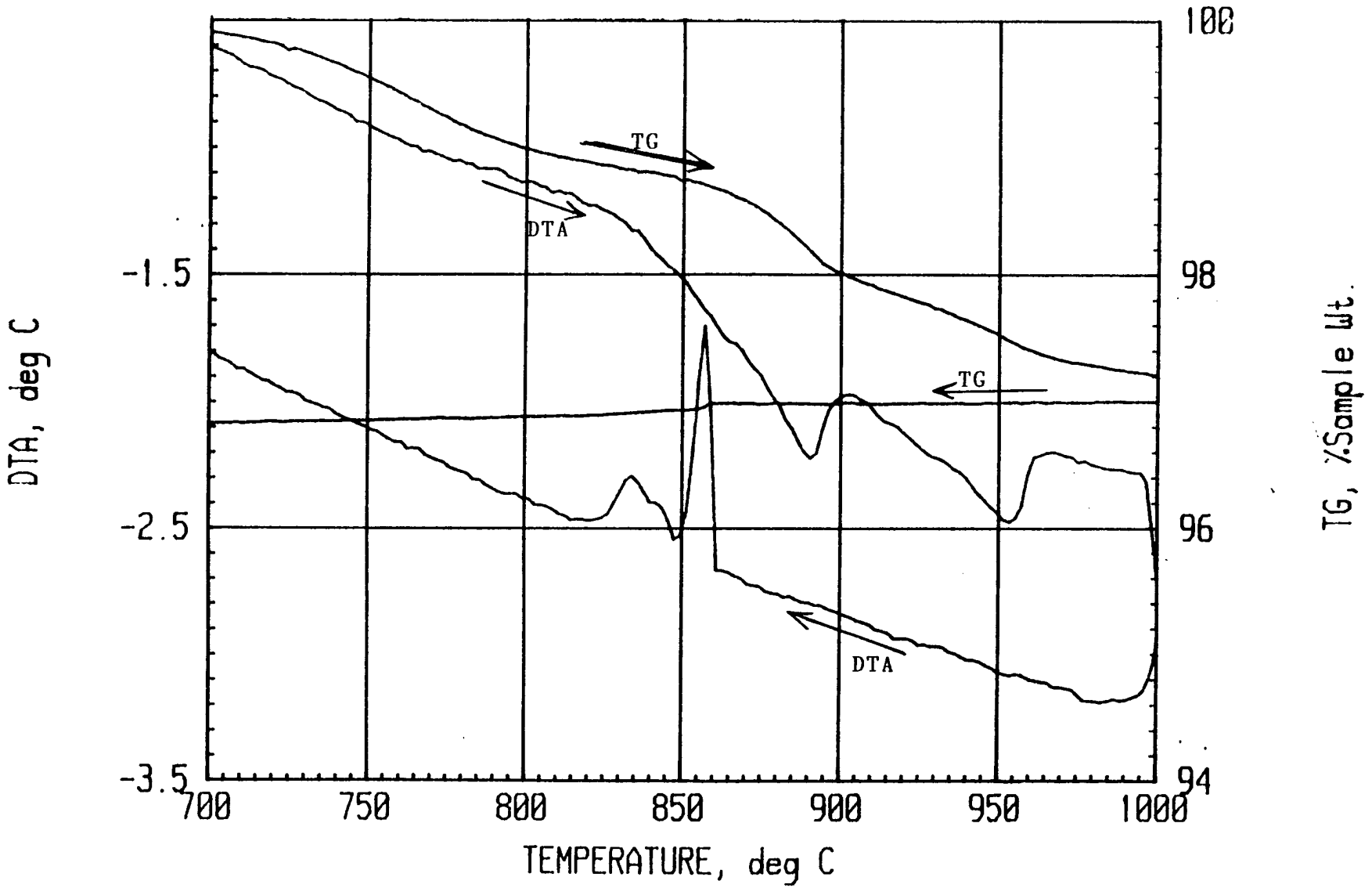

Fig. 4-4. Simultaneous DTA/TG data during the warming and cooling cycles of the synthesis of a nominal 4 : 5 : 9 YBaCuO sample in Ar gas.

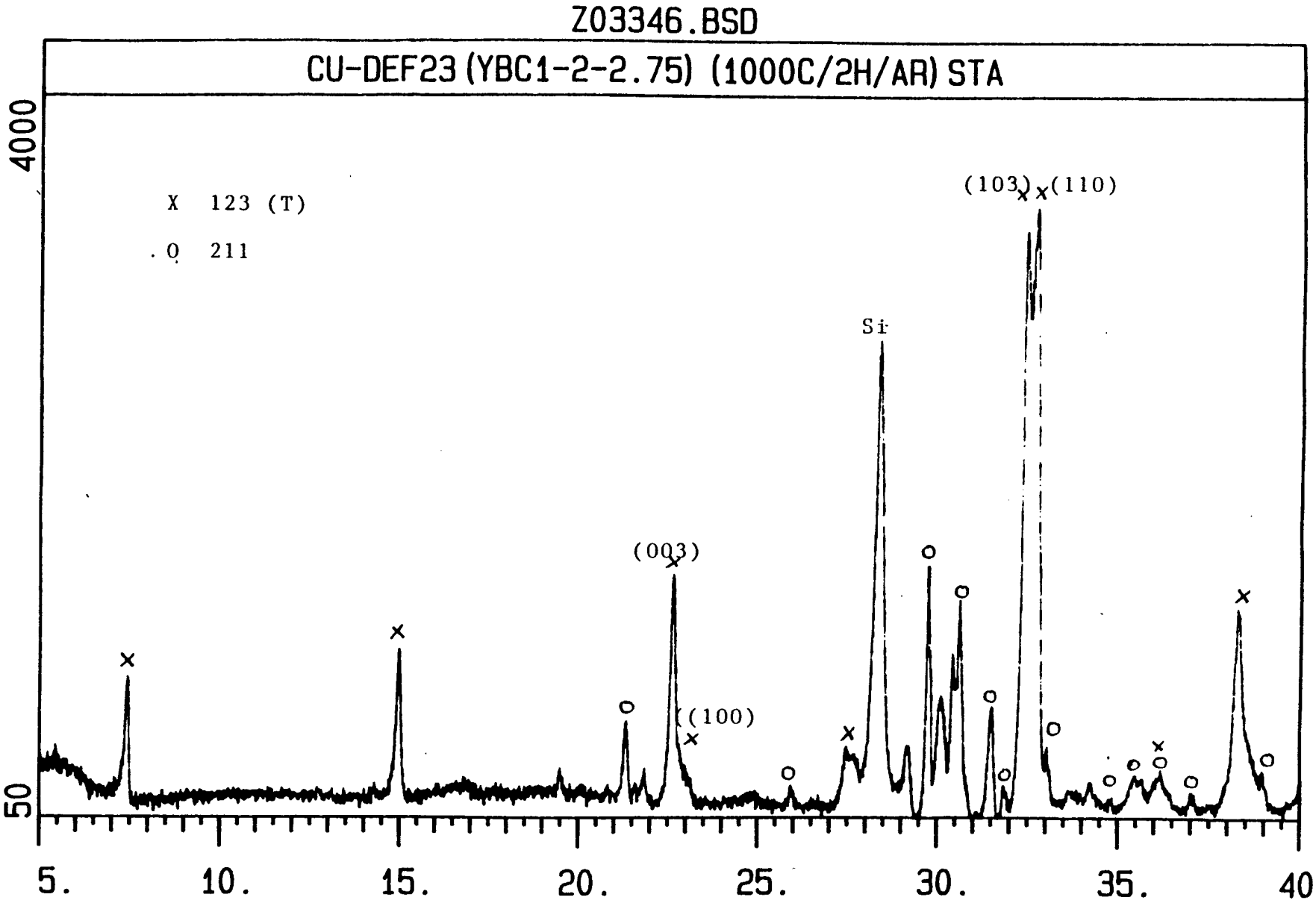

Fig. 4-5. X-ray diffraction pattern for a nominal 1 : 2 : 2.75 YBaCuO sample synthesized at 1000°C in Ar.

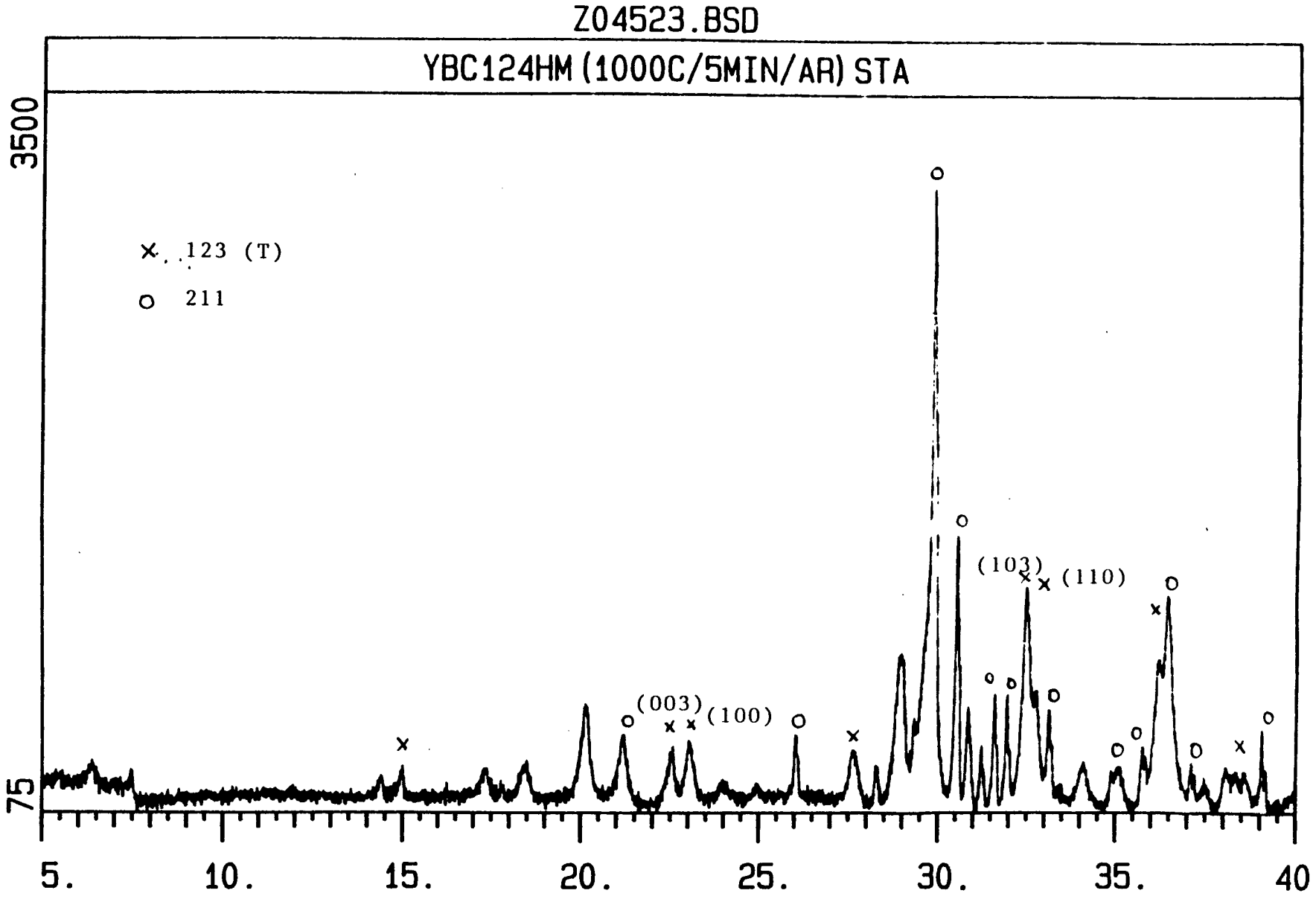

Fig. 4-6. X-ray diffraction pattern for a nominal 1 : 2 : 4 YBaCuO sample synthesized at 1000°C in Ar.

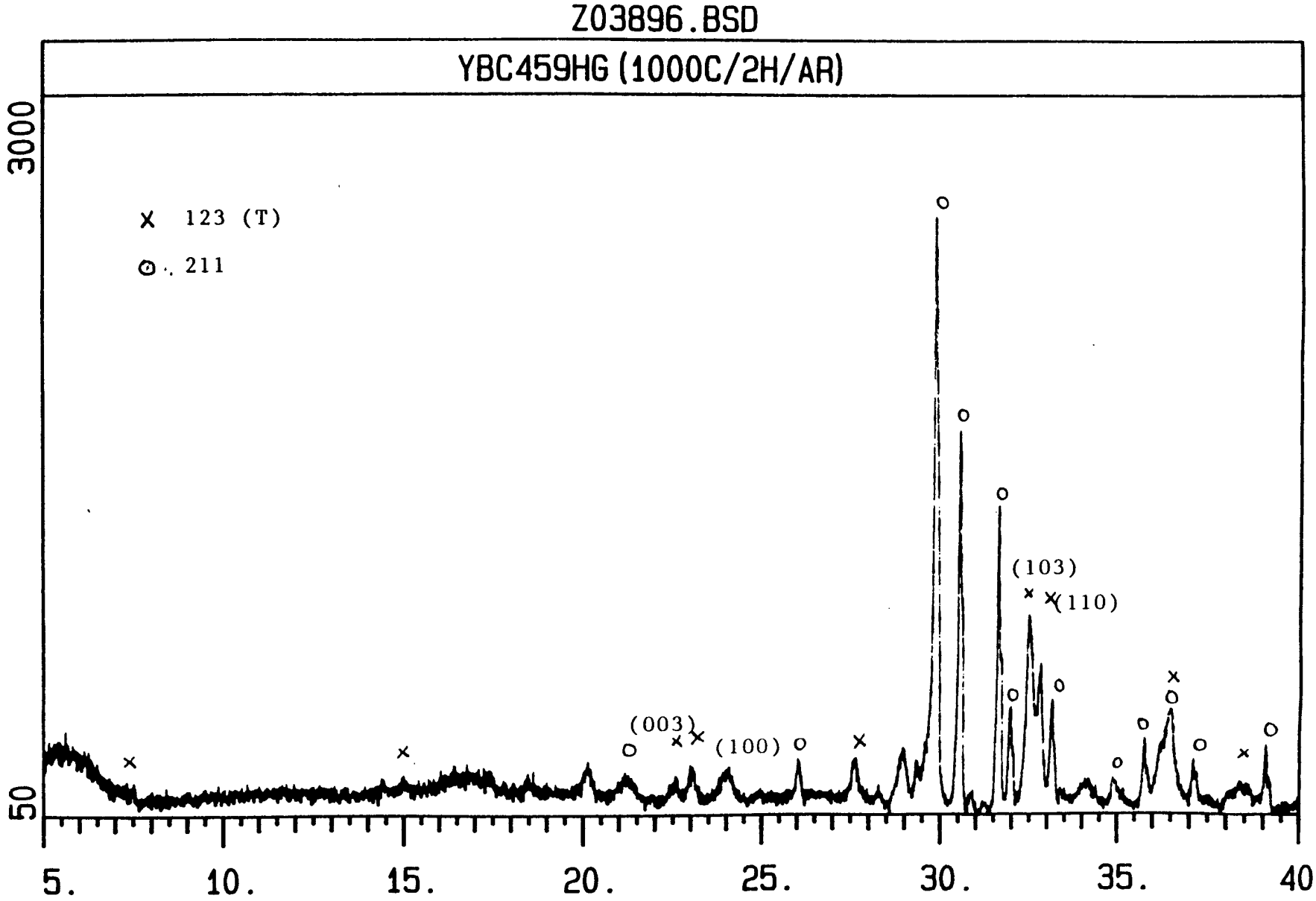

Fig. 4-7. X-ray diffraction pattern for a nominal 4 : 5 : 9 YBaCuO sample synthesized at 1000°C in Ar.

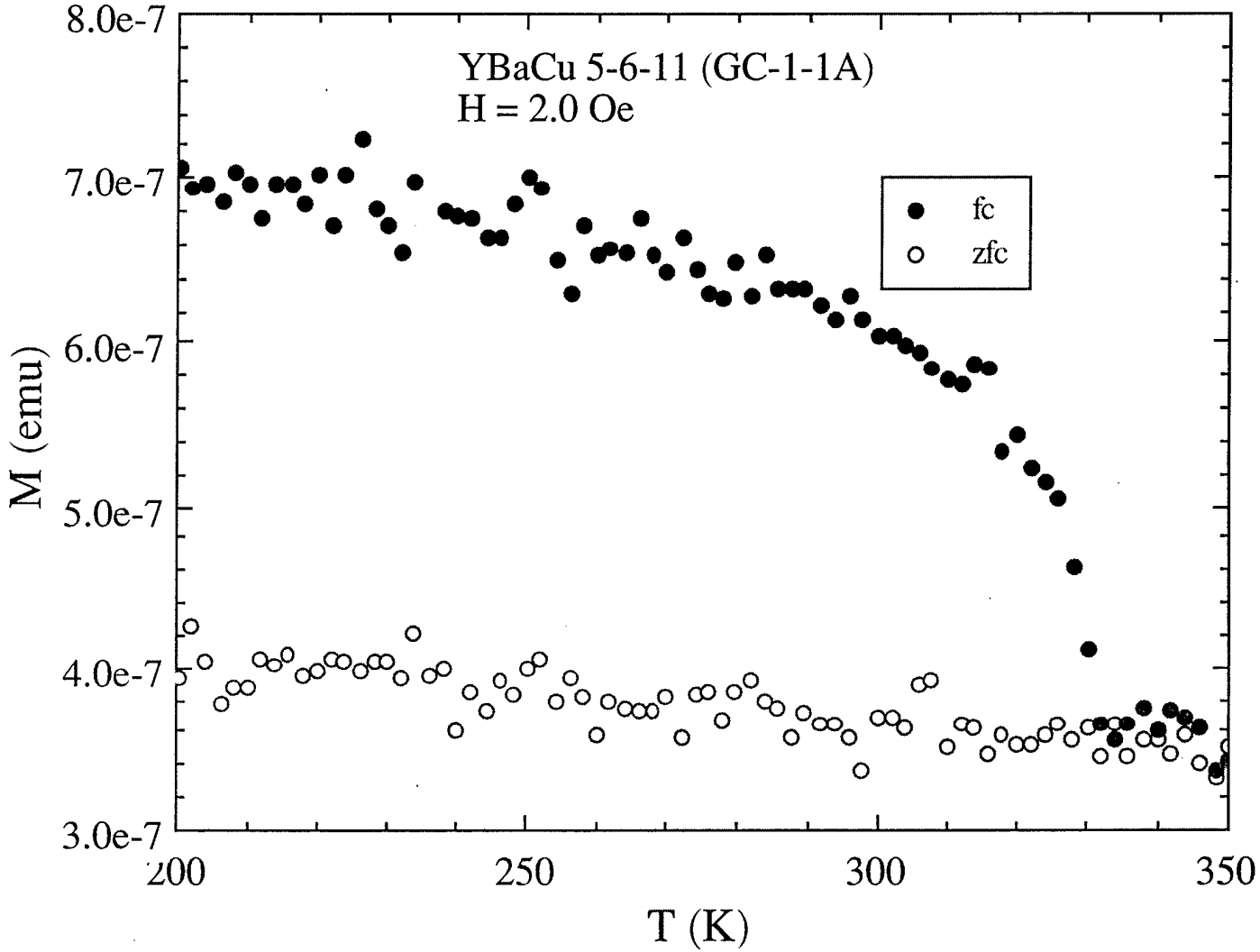

Fig. 4-8. The ZFCM and FCM for a nominal 5:6:11 YBaCuO sample (GC-1-1) for a field of 2 Oe.

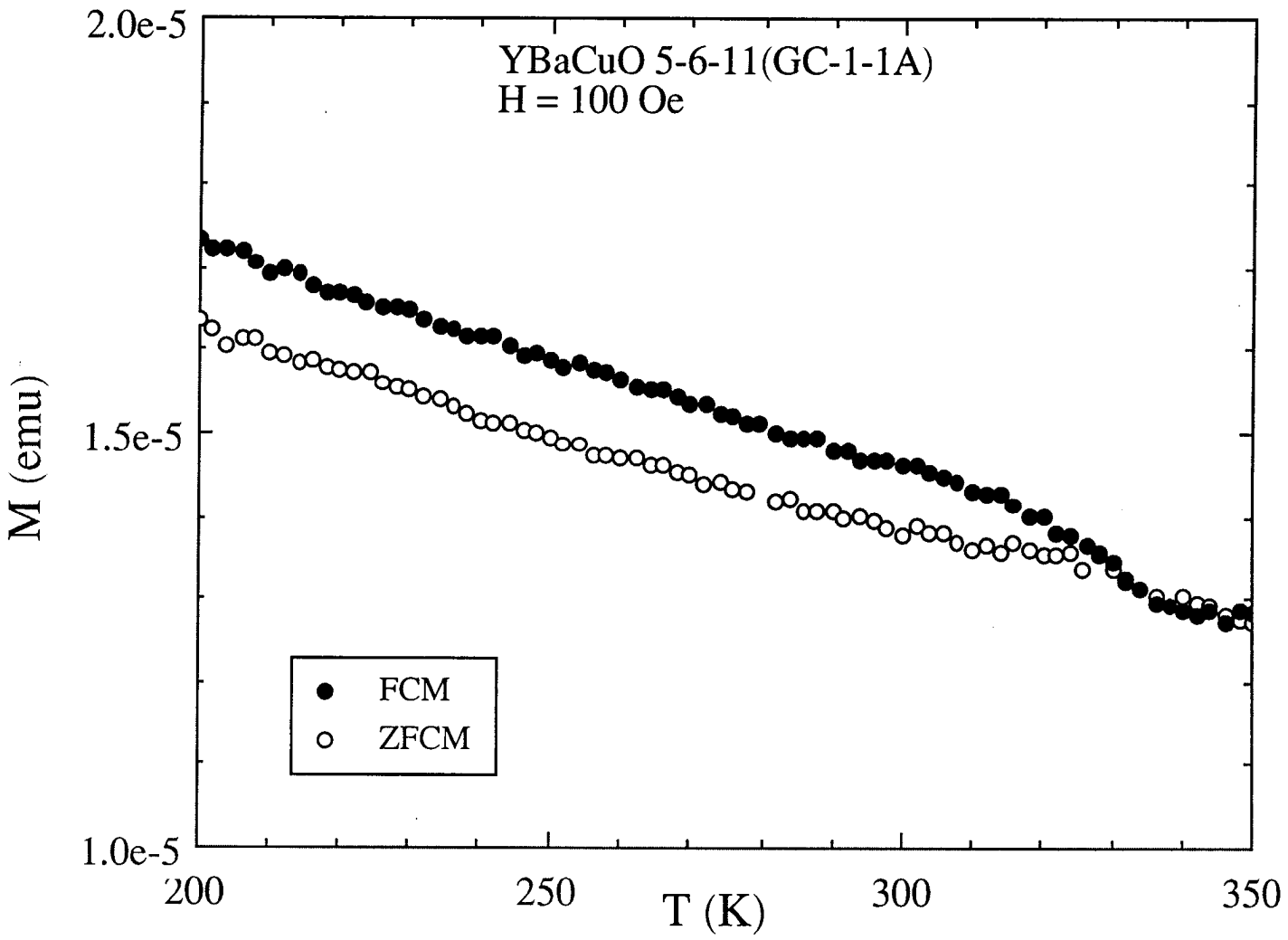

Fig. 4-9. The ZFCM and FCM for a nominal 5:6:11 YBaCuO sample (GC-1-1) for a field of 100 Oe.

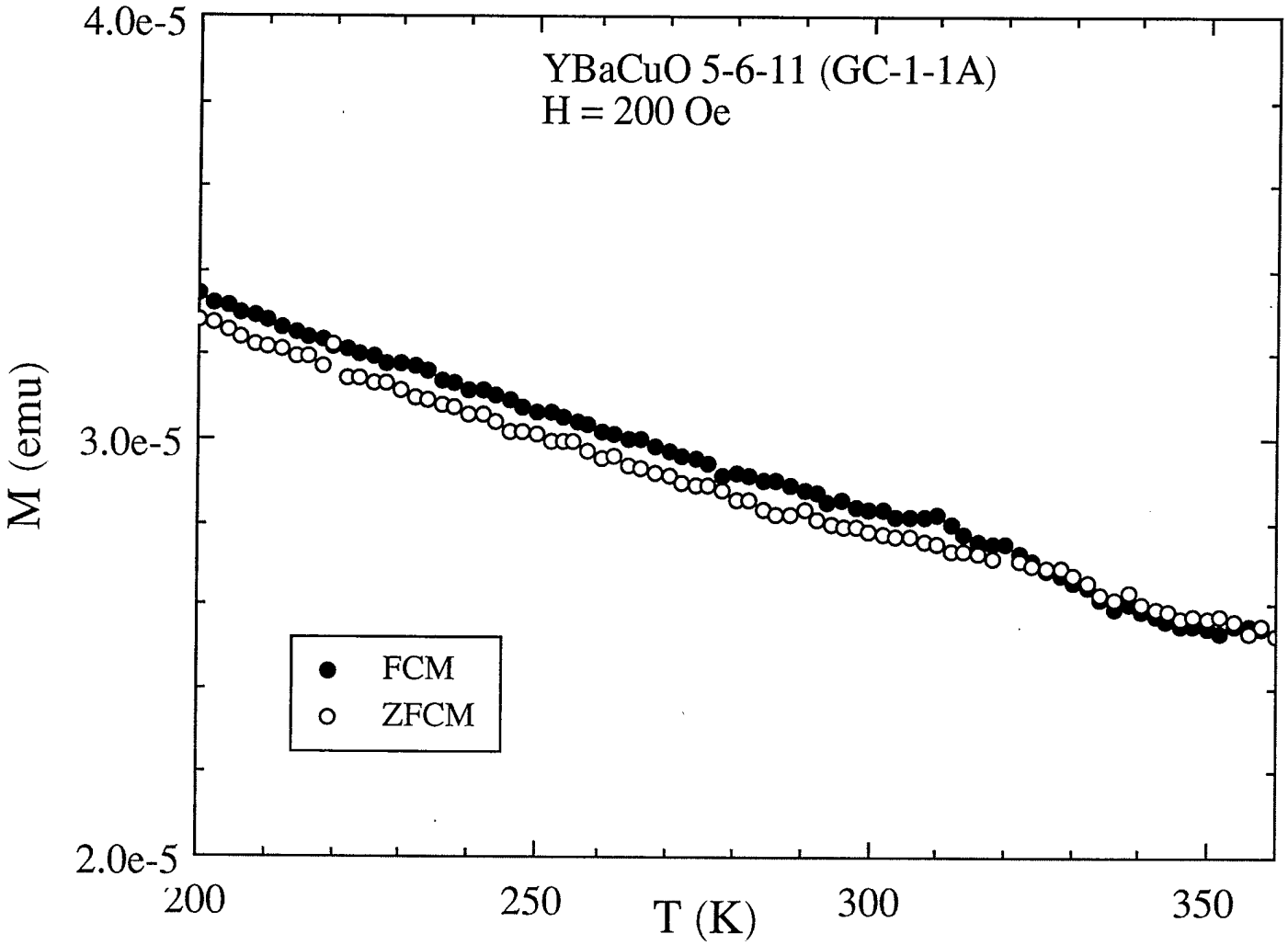

Fig. 4-10. The ZFCM and FCM for a nominal 5:6:11 YBaCuO sample (GC-1-1) for a field of 200 Oe.

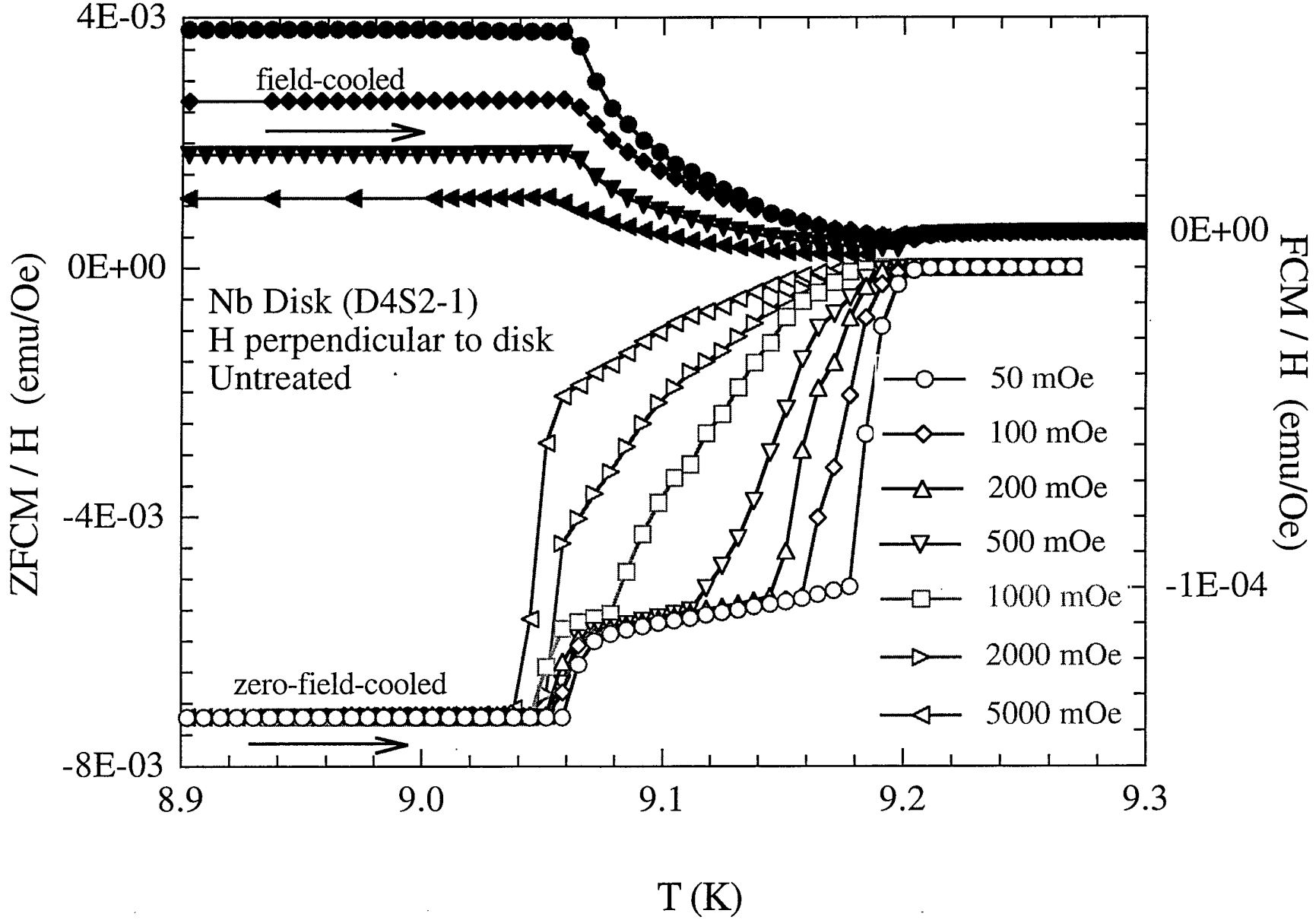

Fig. 5-1. The ZFCM/H (lower) and FCM/H (upper) data for a 0.127-mm thick Nb disk with magnetic fields applied normal to the disk surface.

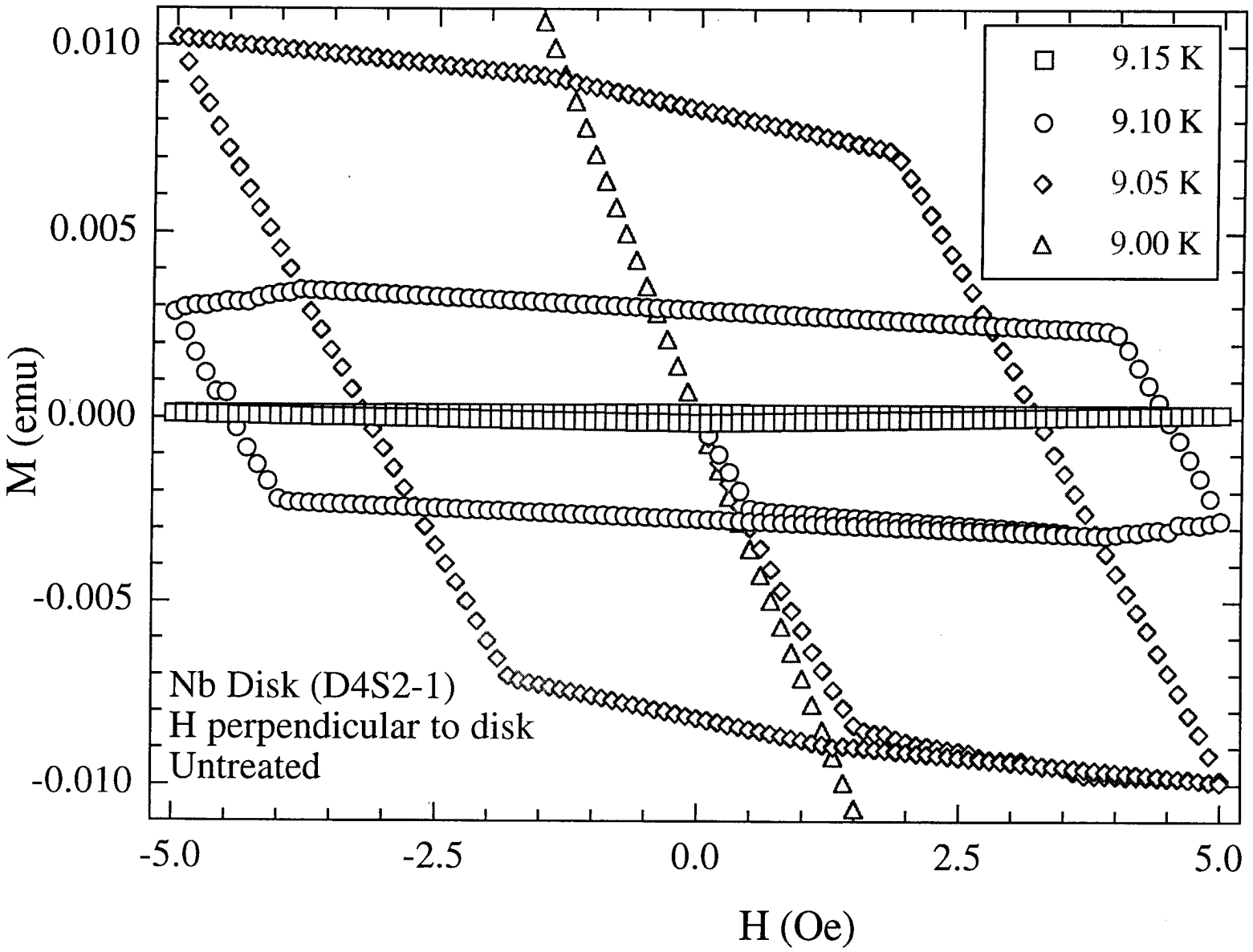

Fig. 5-2. Magnetization versus applied field H curves at various temperatures for H normal to the disk surface.

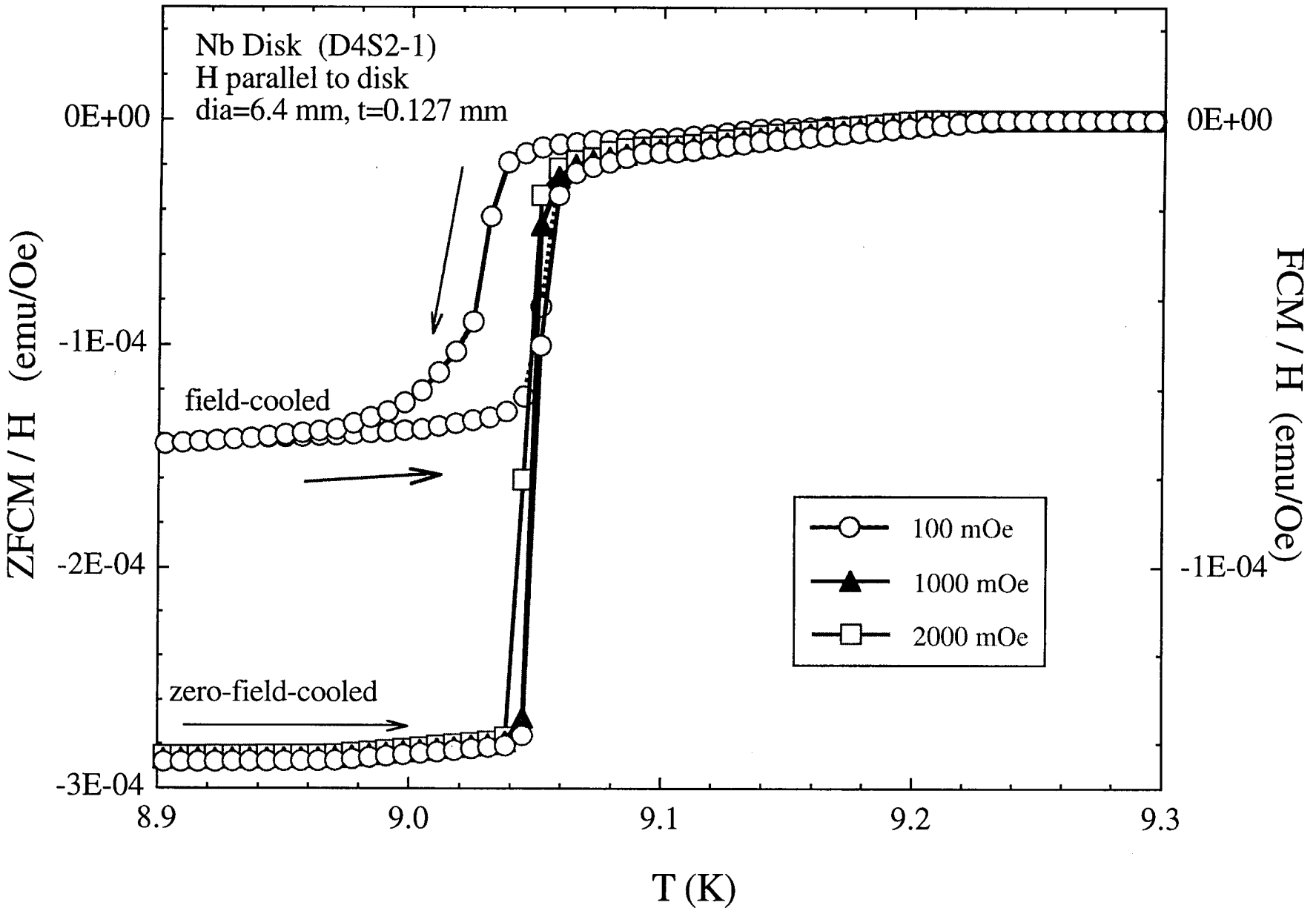

Fig. 5-3. The ZFCM/H (lower) and FCM/H (upper) data for a 0.127-mm thick Nb disk with magnetic fields applied parallel to the disk surface.

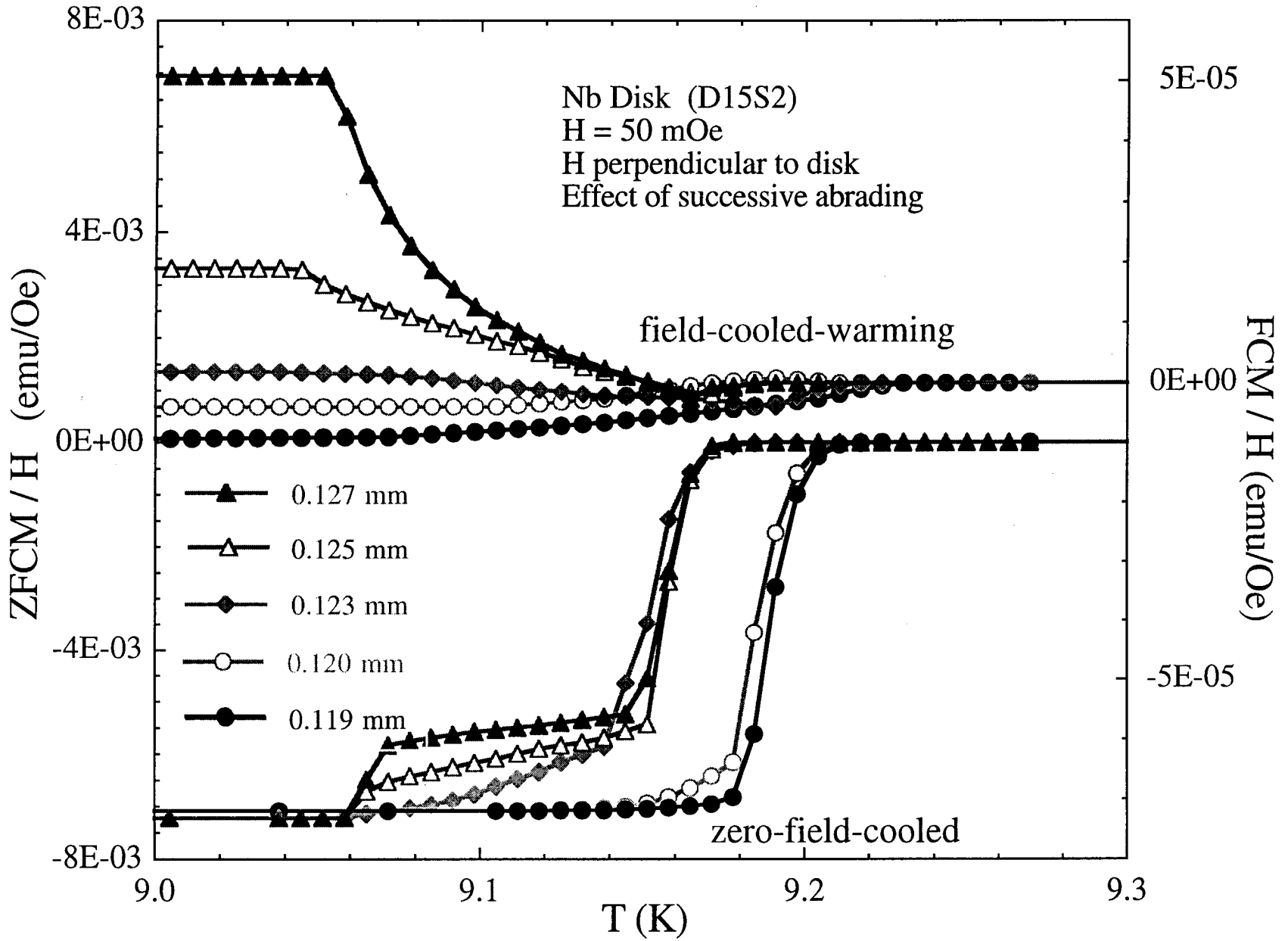

Fig. 5-4. The ZFCM/H (lower) and FCM/H (upper) data for successive surface abrasion of a Nb disk with H normal to the disk surface.

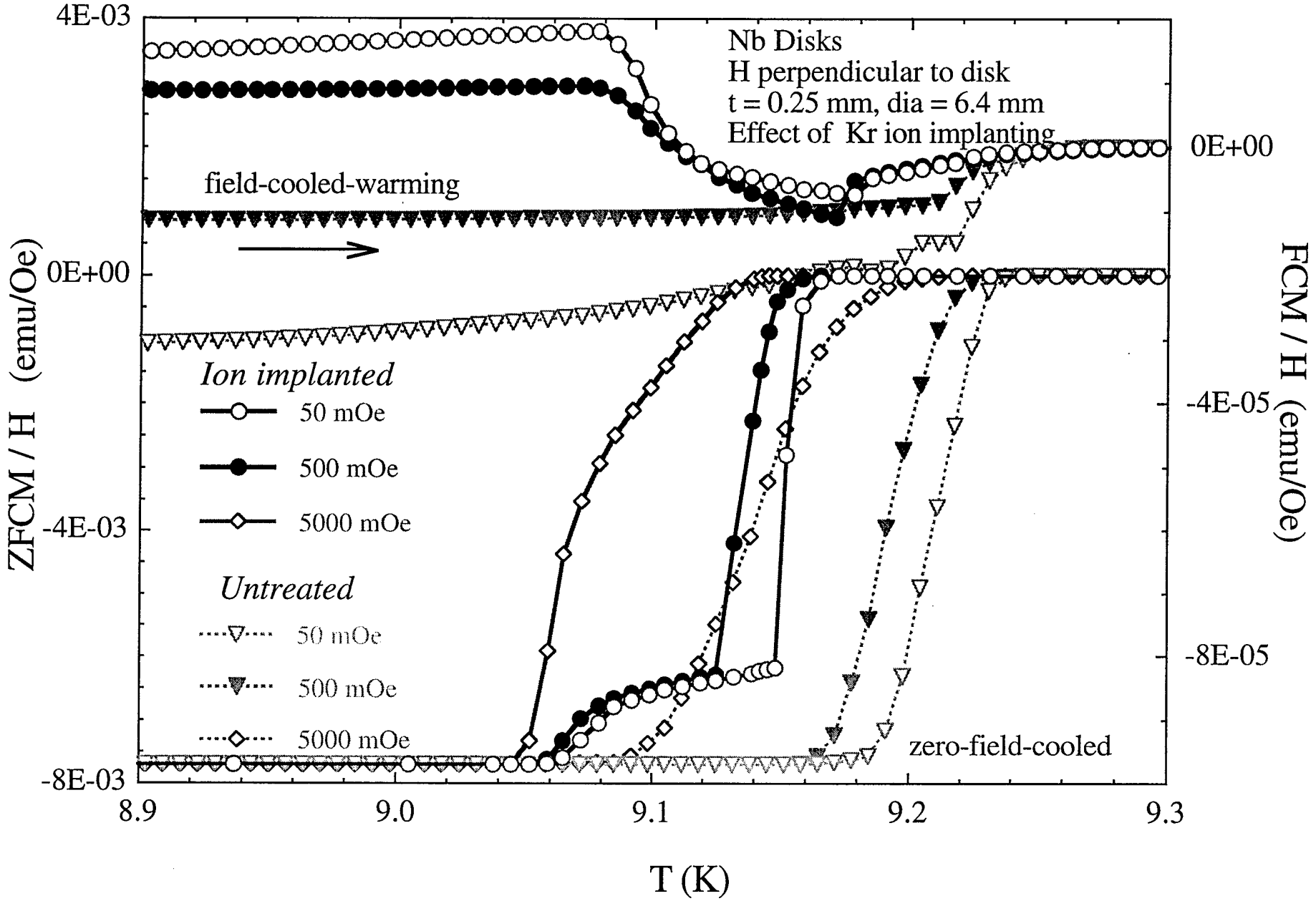

Fig. 5-5. The ZFCM/H (lower) and FCM/H (upper) data for a 0.25-mm thick Nb disk before and after ion implanting with H normal to the disk surface.

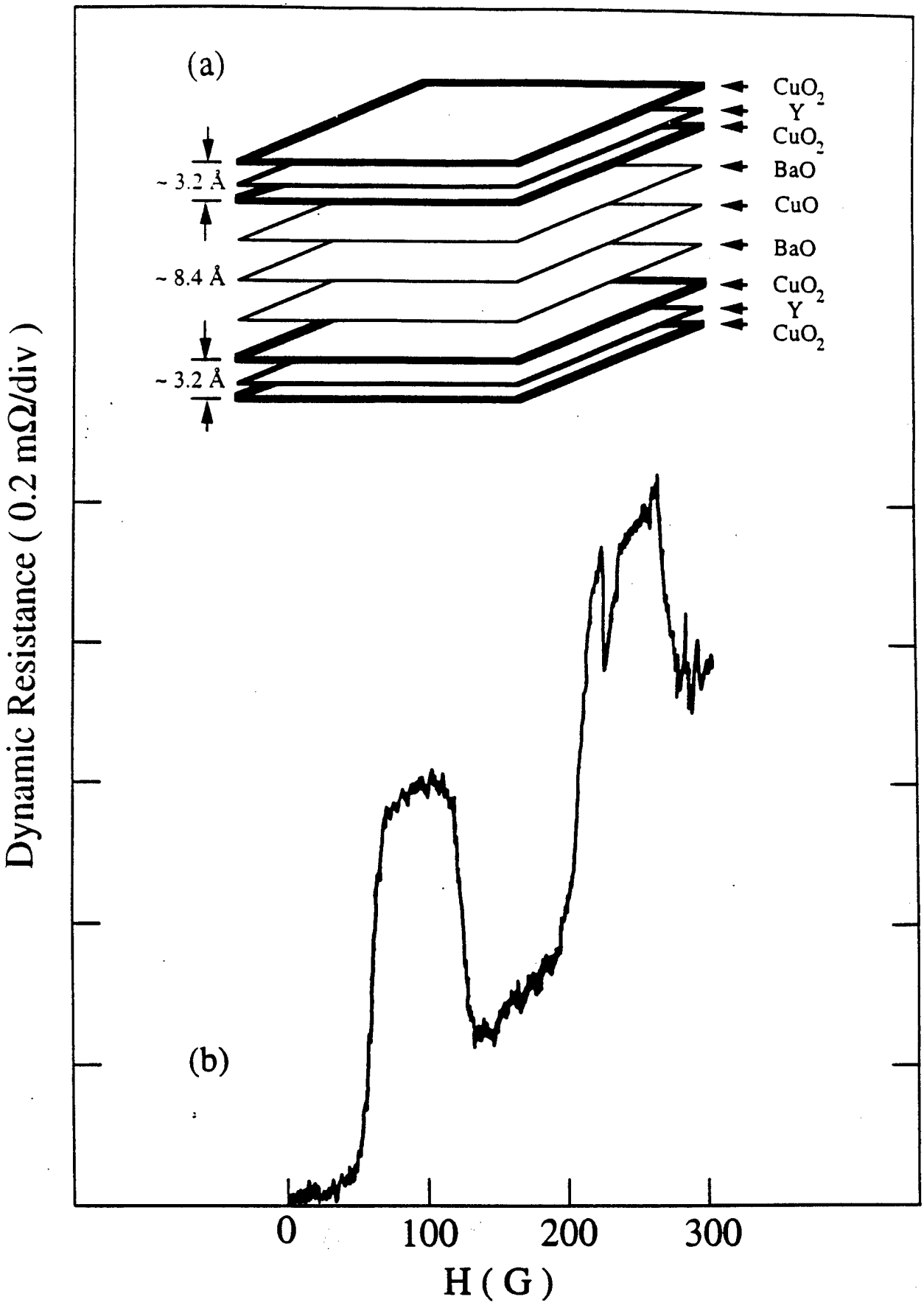

Fig. 6-1. Modulation of the dynamic resistance vs magnetic field at T=80.54 K with ac current along *c* -axis direction and magnetic field parallel to *ab* -plane on a nominal $YBa_2Cu_3O_{7-\delta}$ single crystal sample.

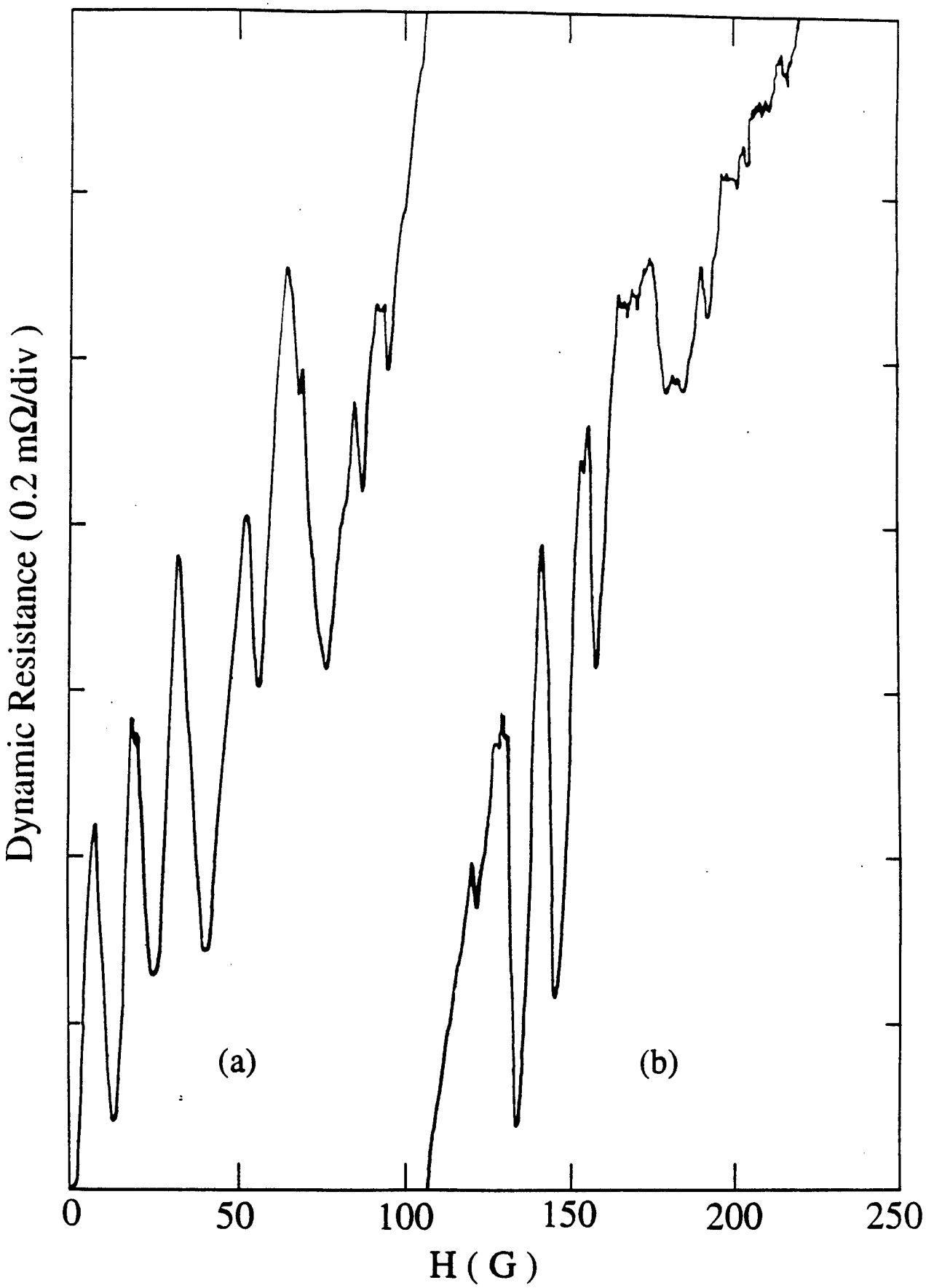

Fig. 6-2. Modulation of the dynamic resistance vs magnetic field at T=79.80 K.

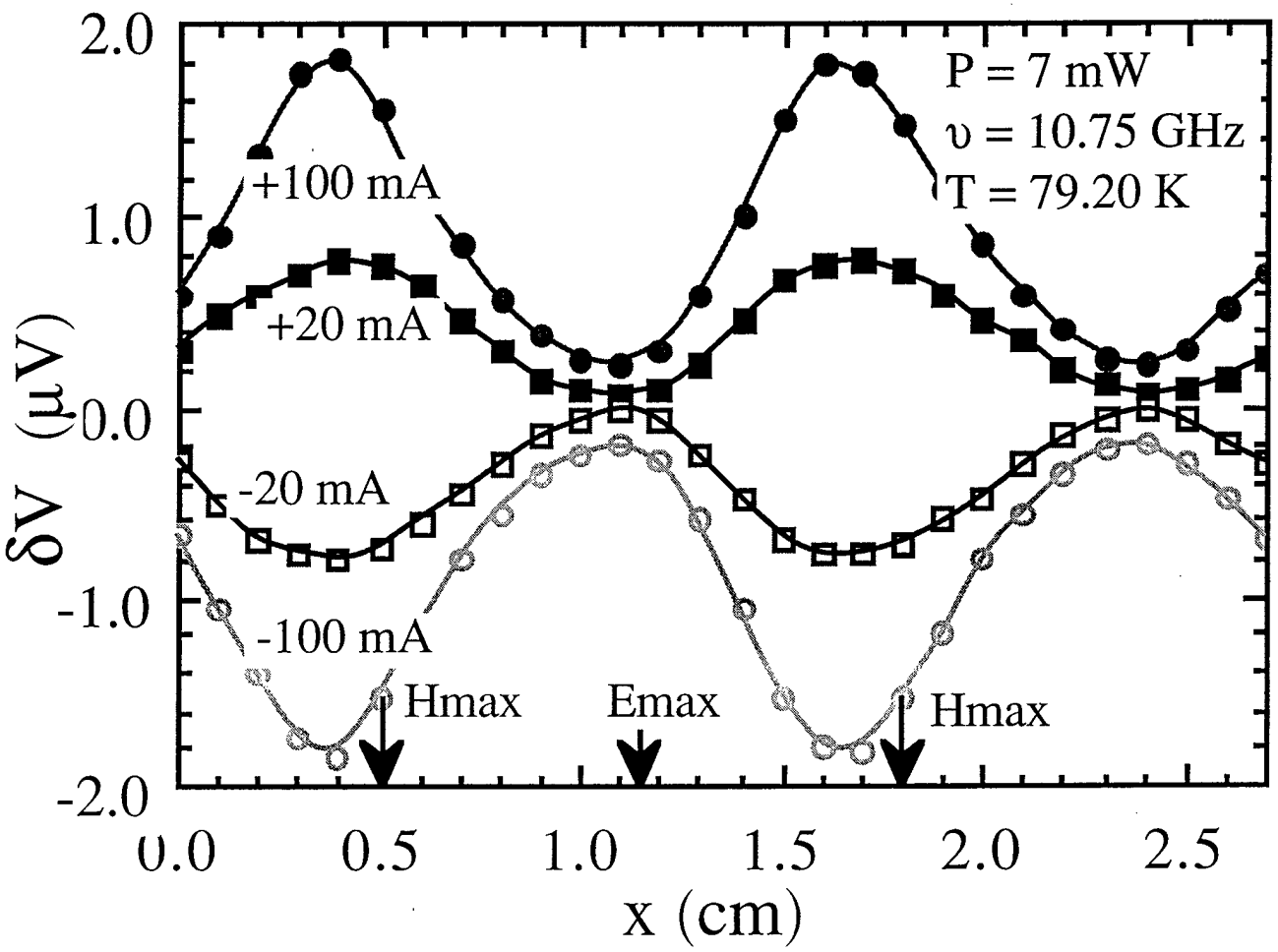

Fig. 6-3. The microwave induced dc voltages vs sample position for different bias currents on a a nominal $YBa_2Cu_3O_{7-\delta}$ single crystal sample.